

Mean and Variance of Brownian Motion with Given Final Value, Maximum and Argmax: Extended Version

Kurt Riedel*

Abstract

The conditional expectation and conditional variance of Brownian motion, $B(t)$, is considered given $B(t=1)$, its maximum and its argmax, $B(t|close, max, argmax)$, as well as those with less information: $B(t|close, argmax)$, $B(t| argmax)$, $B(t| max, argmax)$ where the close is the final value: $B(t = 1) = c$ and $t \in [0, 1]$. We compute the expectation and variance of a Brownian meander in time. By splicing together two Brownian meanders, the mean and variance of the constrained process are calculated. Analytic expressions are given for $E[B(t|close, max, argmax)]$, $E[B(t| max, argmax)]$ and $E[B(t|argmax)]$ as well as the analogous expression for the conditional variance. Computational results displaying both the expectation and variance in time are presented. Comparison of the simulation with theoretical values are shown when the close and argmax are given. We show that using the values of max and argmax as well as the final value, c , significantly reduces the variance of the process compared to the variance of the Brownian bridge.

Keywords: Brownian Motion, Brownian Meander, Brownian Extremum.

AMS MSC 2010: 60J65, 60J70, 91G60.

Submitted to on Stochastic Models on Aug. 27, 2020, revised Feb. 21, 2021, final version accepted on May 31, 2021.

January 22, 2022

1 Introduction

The study of Brownian extrema dates back to Lèvy [14]. We give a brief overview of the results following [7] with additional results taken from [19], [9], [8] and [11]. Our research focuses on distribution of $B(t)$ on $[0, 1]$ given argmax of $B(t)$ and one or more of the maximum and the final value, $B(t = 1) = c$. For each Brownian path on $[0, 1]$, we denote the maximal value of $B(t)$ by h , denoting the “high”. We denote the minimal value, the “low”, by ℓ . The location of the first time when the $B(t)$ reaches h will be denoted by θ (and occasionally by $argmax$). The location of the first time when the $B(t)$ reaches ℓ will be denoted by θ_ℓ . We are interested in the density of Brownian paths conditional on $(c, h, \ell, \theta, \theta_\ell)$. Unfortunately, this five dimensional parameterization is too complex for us to evaluate. Instead, we settle for evaluating the conditional density, $p(x, t|c, \theta, h)$ as well as $p(x, t|\theta, h)$ and $p(x, t|\theta)$. The distribution, $P(x, t|c, \theta, h)$, is well known [20, 6], and has a representation in terms of two Brownian meanders [9, 8, 10, 11, 3]. We do give a more explicit representation of this density in Corollary 4.2. Our companion article [17] examines on $p(x, t|c, h, \ell)$, $p(x, t|c, h)$, $p(x, t|h, \ell)$ and $p(x, t|h)$.

To better understand the conditional probability, we calculate the first and second moments of the probability conditional with respect to x . We evaluate the distribution, mean and variance of $B(t|close, argmax, max)$, $B(t| max, argmax)$ and $B(t|argmax)$. Our companion article [17] examines on $B(t| max)$, $B(t|close, max)$, and $B(t|close, max, min)$. For our results, we view the maximum value, the final value and the location of the maximum, θ , as statistics on the Brownian motion. In other words, given values of (c, h, θ) , we can estimate the properties of a realization of Brownian motion by plugging in the values of these statistics into the density and its first and second moments. The calculation of the moments of $p(x, t|c, \theta, h)$ is new, as is the evaluation of $p(x, t|\theta, h)$ and $p(x, t|\theta)$ and their moments.

By computing the moments, $E[B(t|close, max, argmax)]$ and $Var[B(t|close, max, argmax)]$, we show how the values of (close, high, low, argmax) determine the behavior of $B(t)$ over the entirety of the

*Millennium Partners LLC E-mail: kurt.riedel@gmail.com

region, $[0, 1]$. Both the analytic formulae of the conditional expectation and variance as well as the figures in this paper build intuition about Brownian paths.

Section 2 reviews the distribution of Brownian motion extrema. Section 3 reviews the Brownian meander and calculates its expectation and variance in Theorem 3.3. Section 4 elaborates on Williams's construction [20, 21, 6] of conditional Brownian motion as the splicing together of two Brownian meanders. Theorem 4.3 gives analytic expressions for the expectation and variance of the conditional density, $E[B(t|c, \theta, h)]$ and $Var[B(t|c, \theta, h)]$. Section 5 calculates the density (Theorem 5.1) and moments, $E[B(t|\theta, h)]$ and $Var[B(t|\theta, h)]$, of $B(t|\theta = \text{argmax}, h = \text{max})$. Section 7 and Appendix B describe our simulation framework and compares the simulation with our analytic expressions for the conditional mean and variance. Section 6 presents our analytic $B(t|\text{argmax})$ including expressions for $E[B(t|\theta)]$ and $Var[B(t|\theta)]$. It compares our analytic moments with those of the simulation. We conclude by comparing the time averaged expected variance given one or more of (close, argmax, max, min). In this extended version, we add many more figures of the $E[B(t|parameters)]$ and $Var[B(t|parameters)]$. Appendix C presents the simulation results for the moments of $B(t|\text{max}, \text{argmax})$. We display plots of $E[B(t|\theta, h)]$ and $Var[B(t|\theta, h)]$ as θ and h vary. Appendix D presents similar simulation results for the moments of $B(t|\text{close}, \text{argmax}, \text{max})$. Appendix E concludes simulation results for the moments of $B(t|\text{close}, \text{argmax})$.

2 Distributions of Brownian Extrema

The study of Brownian extrema date back to the founders of the field [14]. Our brief discussion follows [7] with additional results taken from [19, 9, 8, 11, 4]. To our knowledge, there is no known expression for $p(c, h, \ell, \theta, \theta_\ell)$. There are expressions for $p(c, \theta, h)$, $p(c, h, \ell)$, $p(c, h)$, $p(h, \ell)$, $p(h, \theta)$, $p(c, \theta)$ as well as $p(c)$, $p(h)$ and $p(\theta)$.

In [19, 13], the joint density of the close, $B(t = 1) \equiv c$, the high, $\max_{\{t \leq 1\}} B(t) \equiv h$, the location of the high, $\text{argmax}_{\{t \leq 1\}} B(t) \equiv \theta$, is shown to be:

$$p(c, \theta, h) = \frac{h(h-c)}{\pi\theta^{3/2}(1-\theta)^{3/2}} \exp\left(-\frac{h^2}{2\theta} - \frac{(h-c)^2}{2(1-\theta)}\right), \quad h \geq 0, \quad h \geq c. \quad (2.1)$$

Conditional density of θ and h given $B(1)$ is

$$p(\theta, h|B(1) = c) = \frac{h(h-c)\sqrt{2\pi}\exp(c^2/2)}{\pi\theta^{3/2}(1-\theta)^{3/2}} \exp\left(-\frac{h^2}{2\theta} - \frac{(h-c)^2}{2(1-\theta)}\right), \quad h \geq 0, \quad h \geq c. \quad (2.2)$$

The unconditional density of θ and h is obtained by integrating (2.1) on $c < h$ [19, 7, 1]:

$$p(\theta, h) = \frac{1}{\pi} \frac{h \exp(-h^2/2\theta)}{\theta^{3/2}(1-\theta)^{1/2}}, \quad h > 0, \quad 0 < \theta < 1. \quad (2.3)$$

The conditional density of h given θ [19] is

$$p(h|\theta) = \frac{h}{\theta} \exp(-h^2/2\theta), \quad h > 0. \quad (2.4)$$

Thus $E[h|\theta] = \sqrt{\pi\theta/2}$, $Var[h|\theta] = (2 - \pi/2)\theta$. The classic result [14, 12] derived using the reflection principle is the joint distribution of the close, c , the high, h is

$$P(h, c) = P(\max\{B(s), s \in [0, 1]\} \leq h, B(1) = c) = \phi_{\sigma^2}(c) - \phi_{\sigma^2}(2h - c) \quad (2.5)$$

where we denote the Gaussian density by $\phi_{\sigma^2}(x) = (2\pi\sigma^2)^{-1/2} \exp(-x^2/2\sigma^2)$. This result has been generalized to other diffusions in [16]. The marginal density of the maximum, h , and $B(1)$:

$$p(h, c) = \sqrt{\frac{2}{\pi}} (2h - c) \exp(-(2h - c)^2/2), \quad h \geq 0, \quad h \geq c. \quad (2.6)$$

[14, 12]. This can be derived by differentiating (2.6) or by integrating (2.1) over θ .

Let H_c be the random variable $\max_{\{0 < t \leq 1\}} B(t)$ conditional on $B(t=1) = c$. The density of H_c , $p(h|c)$, can be computed using [15, 7]:

$$H_c \equiv \max B(t|B(1) = c) \stackrel{L}{\sim} c/2 + \sqrt{c^2 + 2E}/2 \quad (2.7)$$

where E is a standard exponentially distributed random variable and $\stackrel{L}{\sim}$ means equality in distribution. The marginal density of h is the half normal:

$$p(h) = \sqrt{\frac{2}{\pi}} \exp(-h^2/2), \quad h > 0. \quad (2.8)$$

The marginal density of the location, θ , of the maximum of $B(t)$ is the well-known arcsine distribution, $p(\theta) = \frac{1}{\pi} \frac{1}{\sqrt{\theta(1-\theta)}}$. Using (2.1), one can generate the joint distribution of $(\theta, M, B(1))$ [7] as

$$(\theta, M, B(1)) \stackrel{L}{\sim} \left(\Theta \equiv \frac{1 + \cos(2\pi U)}{2}, \sqrt{2\Theta E}, \sqrt{2\Theta E} - \sqrt{2(1-\Theta)E'} \right). \quad (2.9)$$

An immediate consequence of (2.9) is that the variance of $B(1)$ given θ , the time of the maximum of $B(t)$, is independent of θ and satisfies:

$$\text{Var}[B(1)|\theta] = 2(1 - \pi/4), \quad E[B(1)|\theta] = \sqrt{2} \left(\sqrt{\theta} - \sqrt{1-\theta} \right). \quad (2.10)$$

Here E, E', U are independent random variables where E and E' are standard exponentially distributed and U is uniformly distributed in $[0, 1]$. We are unaware of any previous derivation of this straightforward result. We actually discovered it during our simulation. We now evaluate $p(\theta, c)$. For $c > 0$:

$$p(\theta, c) = \int_c^\infty p(\theta, h, c) dh = \int_c^\infty \frac{h(h-c)}{\pi \theta^{3/2} (1-\theta)^{3/2}} \exp\left(-\frac{h^2}{2\theta} - \frac{(h-c)^2}{2(1-\theta)}\right) dh \quad (2.11)$$

$$= \frac{c\theta e^{-\frac{c^2}{2\theta}}}{\pi \sqrt{\theta(1-\theta)}} - \frac{(c^2-1)e^{-\frac{c^2}{2}} \text{erfc}\left(|c| \sqrt{\frac{(1-\theta)}{2\theta}}\right)}{\sqrt{2\pi}}. \quad (2.12)$$

Here erfc is the complimentary error function, $\text{erfc}(z) = 1 - \text{erf}(z)$. For $c \leq 0$, the same integral over h runs from 0 to ∞ .

$$p(\theta, c) = \frac{|c|(1-\theta)e^{-\frac{c^2}{2(1-\theta)}}}{\pi \sqrt{\theta(1-\theta)}} - \frac{(c^2-1)e^{-\frac{c^2}{2}} \text{erfc}\left(|c| \sqrt{\frac{\kappa\theta}{2}}\right)}{\sqrt{2\pi}}. \quad (2.13)$$

This result corresponds to the conditional density $p(\theta|c)$ in [1].

A result that goes back to L  vy [14, 5], if not earlier, is

Theorem 2.1. *The joint distribution of the close, c , the high, h , and the low, ℓ is*

$$P(c, h, \ell) = P(B(1) = c, \ell \leq \{B(s), s \in [0, 1]\} \leq h) = \sum_{k=-\infty}^{\infty} \phi_{\sigma^2}(c-2k(h-\ell)) - \phi_{\sigma^2}(c-2h-2k(h-\ell)) \quad (2.14)$$

$$= \phi_{\sigma^2}(c) - \sum_{k=0}^{\infty} [\phi_{\sigma^2}(c-2h-2k\Delta) + \phi_{\sigma^2}(c-2\ell+2k\Delta)] + \sum_{k=1}^{\infty} [\phi_{\sigma^2}(c-2k\Delta) + \phi_{\sigma^2}(c+2k\Delta)] \quad (2.15)$$

where $\Delta \equiv (h - \ell)$.

Although (2.14) is classic, (2.15) seems to be new. By refactoring (2.14) into the symmetric form, (2.15), we not only treat h and ℓ symmetrically, but also show that the series is in an alternating form. Here $P(c, h, \ell)$ is a distribution in h, ℓ and a density in c . The density, $p(h, \ell)$ may be found in [17].

3 Brownian Meander and Its Moments

A Brownian meander, $B^{me}(t)$, can be thought of as a Brownian motion restricted to those paths where $B^{me}(t) \geq 0$. Since this is a set of paths with measure zero, we rescale the Brownian paths to get a Brownian meander. Following [2, 8], let $B(t)$ be a Brownian motion, $\tau_1 = \sup\{t \in [0, 1] : B(t) = 0\}$, $\Delta_1 = 1 - \tau_1$, we define the Brownian meander as $B^{me}(t) = |B(\tau_1 + t\Delta_1)|/\sqrt{\Delta_1}$. By $B_c^{me}(t)$, we denote the Brownian meander restricted to $B^{me}(t = 1) = c$. Results for the distribution of meanders can be found in [9, 8, 10, 11, 3]. Brownian meanders at a fixed time, t , are distributed as [10, 7]:

$$B_c^{me}(t) \stackrel{L}{\sim} \sqrt{\left(ct + \sqrt{t(1-t)}N\right) + 2Et(1-t)} \quad , \quad (3.1)$$

where N is a standard normal variable, E is a standard exponentially distributed random variable, and N and E are independent. Equation (3.1) applies for a single fixed time and not for the process, $B(t|B(t=1)=c)$ for all $t \leq 1$. We are more interested in the transition density of the meander. Following [8], let $\phi_s(x) = (2\pi s)^{-1/2} \exp(-x^2/2s)$, $N_x(a, b) = \int_a^b \phi_s(x) dx$, then

Theorem 3.1. [8, 10] B^{me} has transition density: $p(B^{me}(t) = y) = 2yt^{-3/2} \exp(-y^2/2t)N_{1-t}(0, y)$ for $0 \leq t \leq 1, y > 0$. For $0 < s < t \leq 1, x, y > 0$,

$$p(B^{me}(t) = y|B^{me}(s) = x) = g_{t-s}(x, y)N_{1-t}(0, y)/N_{1-s}(0, x) \quad , \quad (3.2)$$

$$g_t(x, y) \equiv \phi_t(y - x) - \phi_t(y + x) \quad . \quad (3.3)$$

$P(B^{me}(1) \leq x) = 1 - \exp(-x^2/2)$ is the Rayleigh distribution.

In (3.2), we slightly abuse notation: The probability that $B^{me}(s) = x$ is infinitesimally small and is a density in x : $p(B^{me}(t) = y|B^{me}(s) = dx) = p(B^{me}(t) = y|B^{me}(s) = x)dx$. With this understanding, we will continue to write the conditional densities without dx . The Bayesian Rule gives the conditional density given the final value of a Brownian meander:

Corollary 3.2. [7] For $0 < s < t \leq 1, x, c > 0$, B^{me} has density:

$$p(B^{me}(s) = x|B^{me}(t) = c) = p(B^{me}(t) = c|B^{me}(s) = x)p(B^{me}(s) = x)/p(B^{me}(t) = c) \quad (3.4)$$

$$= g_{t-s}(x, c) \frac{xt^{3/2}}{cs^{3/2}} \exp(-x^2/2s) \exp(c^2/2t) = g_{t-s}(x/\mu, \mu c) \frac{xt^{3/2}}{cs^{3/2}}$$

where $\mu \equiv \sqrt{s/t}$. For $t = 1$, (3.4) can be rewritten as $p(B^{me}(s) = x|B^{me}(t) = c) = g_{s(1-s)}(x, c') \frac{x}{c'}$.

Equivalent formulae to (3.4) are found in [7]. In Appendix A, we calculate the expectation and variance of the Brownian meander using this transition density:

Theorem 3.3. For the Brownian meander, $B^{me}(t)$, the first and second moments are

$$M_1(s, t, c) = \int_0^\infty xp(B^{me}(s) = x|B^{me}(t) = c)dx \quad (3.5)$$

$$= \frac{[t-s+sc^2/t]\text{erf}(\frac{c\sqrt{s}}{\sqrt{2t(t-s)}})}{c} + \frac{\sqrt{2s(t-s)}}{\sqrt{\pi t}} \exp(-sc^2/2t(t-s)) \quad , \quad (3.6)$$

$$M_2(s, t, c) = \int_0^\infty x^2p(B^{me}(s) = x|B^{me}(t) = c)dx = \frac{3s(t-s)}{t} + c^2s^2/t^2 \quad . \quad (3.7)$$

Proof: These formulae are derived in Appendix A using the transition density (3.4).

Theorem 3.3 is new and is the basis for the moment calculations in the remainder of the article. If $t = 1$, we often suppress the third argument: $M_1(s, c) = M_1(s, c, t = 1)$. The variance of the meander satisfies: $Vr(s, c) = M_2(s, c, t = 1) - M_1(s, c, t = 1)^2$. Thus, $Vr(s, c)$ is the variance of a Brownian meander when the end time, $t = 1$ with final value c .

4 Spliced Brownian Meander Representation and Its Moments

Following Williams, [20, 21, 6, 7], we represent a Brownian motion on $[0, 1]$ given the location, θ , its maximum, h and its final value c . We represent $B(t)$ in $[0, \theta]$ in terms of a meander $B^{me}(t)$:

Theorem 4.1. *Consider a Brownian motion conditional on $h = \max_{0 \leq s \leq 1} \{B(s)\}$, θ is the smallest s such that $B(\theta) = h$ and $B(1) = c$. For a fixed time t , $B(t|c, \theta, h)$ is distributed as a scaled Brownian meander to the left of θ and a second scaled Brownian meander to the right of θ .*

$$B(t|c, \theta, h) \stackrel{L}{\sim} h - \sqrt{\theta} B_r^{me}(1 - t/\theta) \text{ for } t \leq \theta \text{ where } r \equiv h/\sqrt{\theta} . \quad (4.1)$$

Here $B_r^{me}(t)$ is the meander process with $B_r^{me}(t = 1) = r$ and $r \equiv h/\sqrt{\theta}$. Similarly for $t \in [\theta, 1]$, define

$$B(t|c, \theta, h) \stackrel{L}{\sim} h - \sqrt{1 - \theta} \tilde{B}_q^{me}\left(\frac{t - \theta}{1 - \theta}\right) \text{ for } t \geq \theta \text{ where } q \equiv \frac{h - c}{\sqrt{1 - \theta}} \quad (4.2)$$

and \tilde{B}_q^{me} is an independent Brownian meander.

The formal proof may be found in [20, 21, 6]. The result is easy to understand: A Brownian meander, $B_c^{me}(t)$, is equivalent to a Brownian bridge restricted to non-negative paths. On either side of the first maximum, θ , the Brownian paths are restricted to not go above the maximum. Thus on either side of θ , we subtract off the appropriately scaled Brownian meander.

A rigorous notation would replace $B(t|c, \theta, h)$ with $B(t|dc, d\theta, dh)$. Theorem 4.1 is well known and sometimes called the Williams representation. We need a more explicit representation to calculate the moments. We now derive it using the meander density representation of the previous situation. We believe the following corollary is more explicit than previous analyses.

Corollary 4.2. *Under the assumptions of Theorem 4.1, the conditional density of a Brownian motion at a fixed time, t , satisfies*

$$p(B(t) = x|c, \theta, h) = g_t(h - x, h) \frac{\theta^{1.5}(h - x)}{(\theta - t)^{1.5}h} \exp\left(\frac{h^2}{2\theta}\right) \exp\left(\frac{-(h - x)^2}{2(\theta - t)}\right) \text{ for } t < \theta . \quad (4.3)$$

For $t > \theta$:

$$p(B(t) = x|c, \theta, h) = g_{1-t}(h - x, h - c) \frac{(h - x)(1 - \theta)^{1.5}}{(h - c)(t - \theta)^{1.5}} \exp\left(\frac{-(h - x)^2}{2(t - \theta)}\right) \exp\left(\frac{(h - c)^2}{2(1 - \theta)}\right) . \quad (4.4)$$

For $t \leq \theta$, the joint density satisfies

$$p(B(t) = x, \theta, h, c) = \frac{(h - c)(h - x)}{\pi(1 - \theta)^{1.5}(\theta - t)^{1.5}} g_t(h - x, h) \exp\left(\frac{-(h - x)^2}{2(\theta - t)} - \frac{(h - c)^2}{2(1 - \theta)}\right) \quad (4.5)$$

where $t \leq \theta$. For $t > \theta$, the joint density is

$$p(B(t) = x, \theta, h, c) = \frac{h(h - x)}{\pi\theta^{1.5}(t - \theta)^{1.5}} g_{1-t}(h - x, h - c) \exp\left(\frac{-(h - x)^2}{2(t - \theta)} - \frac{h^2}{2\theta}\right) . \quad (4.6)$$

Proof: To prove (4.3) and (4.4), we insert the transition density of (3.4) into the results of Theorem 4.1. To prove (4.5), we multiply (4.3) by $p(\theta, h, c)$ from (2.1). To prove (4.6), we multiply (4.4) by $p(\theta, h, c)$. \square

Using (4.1) and (3.7), we calculate the moments of the conditional Brownian motion:

Theorem 4.3. *Under the assumptions of Theorem 4.1, the expectation of a Brownian motion satisfies $E[B(t)|c, h, \theta]$.*

$$E[B(t)|c, \theta, h] = h - \sqrt{\theta} M_1\left(1 - \frac{t}{\theta}, \frac{h}{\sqrt{\theta}}\right) = \quad (4.7)$$

$$h - \sqrt{\theta} \left[\frac{t}{h\sqrt{\theta}} + \frac{h(\theta - t)}{\theta^2} \right] \operatorname{erf}\left(\frac{h\sqrt{\theta - t}}{\sqrt{2t\theta}}\right) + \frac{\sqrt{2t(\theta - t)}}{\sqrt{\pi\theta}} \exp\left(\frac{-(\theta - t)h^2}{2t\theta}\right) \quad (4.8)$$

for $t \leq \theta$. For $t \geq \theta$, the expectation satisfies:

$$E[B(t)|c, \theta, h] = h - \sqrt{1-\theta} M_1\left(\frac{t-\theta}{1-\theta}, \frac{h-c}{\sqrt{1-\theta}}\right) \text{ for } t \geq \theta. \quad (4.9)$$

For $t \leq \theta$, $E[B^2(t)|c, \theta, h] = h^2 - 2h\sqrt{\theta} M_1(s, \frac{h}{\sqrt{\theta}}) + \theta M_2(s, \frac{h}{\sqrt{\theta}})$. Thus the variance satisfies

$$Var[B(t)|c, \theta, h] = \theta Vr(1 - \frac{t}{\theta}, \frac{h}{\sqrt{\theta}}) \text{ for } t \leq \theta, \quad (4.10)$$

$$Var[B(t)|c, \theta, h] = (1-\theta) Vr(\frac{t-\theta}{1-\theta}, \frac{h-c}{\sqrt{1-\theta}}) \text{ for } t \geq \theta, \quad (4.11)$$

where $Vr(s, c) \equiv M_2(s, c) - M_1(s, c)^2 = 3s(1-s) + c^2 s^2 - M_1(s, c)^2$.

Proof: In the representations, (4.1) and (4.2), the conditional density of the Brownian motion (on either side of the argmax, θ), is a linear transformation of the Brownian meander density. Thus the moments of the conditional density, (4.4) and (4.3), are linear transformations of the Brownian meander moments given in Theorem 3.3. The representations in (4.7) - (4.11) follow by substituting the appropriate transformations of the Brownian meander moments into (4.1) - (4.2).

5 Moments Given High and Its Location

To calculate the expectation of $B(t)$ given only its maximum and the first location of its maximum, we integrate the expressions in (4.3) and (4.4) over the correct conditional probability density given by (2.1) and (2.3):

$$p(x, t|\theta, h) = \int_{-\infty}^h p(x, t|c, \theta, h) p(\theta, h, c) dc / p(\theta, h). \quad (5.1)$$

Theorem 5.1. The conditional density, $p(B(s) = x|\theta, h)$ satisfies

$$p(B(s) = x|\theta, h) = \frac{(h-x)}{\pi(1-\theta)^{\frac{1}{2}}(\theta-s)^{1.5}} g_s(h-x, h) \exp\left(\frac{-(h-x)^2}{2(\theta-s)}\right) \quad (5.2)$$

for $t < \theta$. Here $g_{1-s}(x, y) = \phi_{1-s}(x-y) - \phi_{1-s}(x+y)$. For $t > \theta$, the conditional density is

$$p(B(s) = x|\theta, h) = \frac{h(h-x)}{\pi\theta^{1.5}(s-\theta)^{1.5}} \operatorname{erf}\left(\frac{h-x}{\sqrt{2(1-s)}}\right) \exp\left(\frac{-(h-x)^2}{2(s-\theta)} - \frac{h^2}{2\theta}\right). \quad (5.3)$$

Proof: We integrate (4.5) and (4.6) with respect to the close, c and then divide by $p(\theta, h)$ as given by (2.3). We use $\int_{-\infty}^h g_{1-s}(z, h-c) dc = \int_0^\infty \phi_{1-s}(x-z) - \phi_{1-s}(x+z) dx = \operatorname{erf}\left(\frac{z}{\sqrt{2(1-s)}}\right)$. \square

To calculate the expectation of $B(t)$ given only its maximum and the first location of its maximum, we need only integrate the expressions in (3.5) - (4.9) over the same conditional probability density:

$$E[B(t|\theta, h)] = \int_{-\infty}^h E[B(t)|c, \theta, h] p(\theta, h, c) dc / p(\theta, h) \quad (5.4)$$

where $p(\theta, h, c)$ is given by (2.1) and $p(\theta, h)$ is given by (2.3). Thus $p(\theta, h, c)/p(\theta, h) = \frac{(h-c)}{(1-\theta)} \exp(\frac{-(h-c)^2}{2(1-\theta)})$. We change variables from c to $x \equiv \frac{(h-c)}{\sqrt{1-\theta}}$ and apply (9.13) - (9.15) the Appendix A.

Theorem 5.2. For $t > \theta$, the expectation becomes

$$E[B(t|\theta, h)] = h - \sqrt{1-\theta} \int_0^\infty x M_1(s, x) e^{-x^2/2} dx = h - \sqrt{1-\theta} G_{11}(s), \quad (5.5)$$

where $s \equiv \frac{t-\theta}{1-\theta}$ and $G_{11}(s)$ is defined as

$$G_{11}(s) = \sqrt{\frac{2}{\pi}} \left[\tan^{-1}\left(\sqrt{\frac{s}{1-s}}\right) + \sqrt{s(1-s)} \right]. \quad (5.6)$$

Thus $E[B(t|\theta, h)] - h$ is independent of h for $t \geq \theta$. For $t \leq \theta$, $E[B(t)|c, \theta, h]$ is independent of c and satisfies $E[B(t)|\theta, h] = E[B(t)|c, \theta, h]$ as given by (4.7) - (4.8). For $t \leq \theta$, the variance is independent of the close and is given by (4.10):

$$\text{Var}[B(t|\theta, h)] = \theta \text{Var}(1 - \frac{t}{\theta}, \frac{h}{\sqrt{\theta}}) \quad \text{for } t \leq \theta . \quad (5.7)$$

For $t \geq \theta$, the variance of $B(t|\theta, h)$

$$\text{Var}[B(t|\theta, h)] = (1 - \theta)[3s - s^2] - (1 - \theta)G_{11}(s)^2 . \quad (5.8)$$

Proof: The proof of (5.5) is in (9.13) - (9.15). The variance of $B(t|\theta, h)$ is calculated by the ensemble average of $E[B^2(t|c, \theta, h)]$ and subtracting $E[B(t|\theta, h)]^2$. For $t \leq \theta$, $E[B(t)^2|c, \theta, h]$ is also independent of c . This proves (5.7). For $t \geq \theta$,

$$\text{Var}[B(t|\theta, h)] = \int_{-\infty}^h E[B^2(t|c, \theta, h)]p(c|\theta, h)dc - E[B(t|\theta, h)]^2 \quad (5.9)$$

$$= h^2 - 2\sqrt{(1 - \theta)h}E[B(t|\theta, h)] + (1 - \theta) \int_0^\infty x M_2(s, x) e^{-\frac{x^2}{2}} dx - E[B(t|\theta, h)]^2 . \quad (5.10)$$

To evaluate (5.10), we insert (9.16) and (5.5) into (5.10). \square

By ignoring the c dependence in $B(t|c, \theta, h)$, the variance increases by $\int_{-\infty}^h E[B(t|c, \theta, h)]^2 p(c|\theta, h)dc - E[B(t, \theta, h)]^2$. One can think of this as an Analysis of Variance term. The increase occurs because the final value, c , is now a random variable.

Similar but more complicated moment calculations are possible for the case of the previous section where (θ, c) are given and one integrates over h . In [17], analytic expressions for $E[B(t|c, h)]$ and $\text{Var}[B(t|c, h)]$ are given. It may be possible to rederive these results by integrating $p(x, t|c, \theta, h)p(\theta, h, c)d\theta/p(c, h)$. This integration appears to be untractable.

6 Mean and Variance Given Only Argmax

Now consider $B(t|\text{argmax } B = \theta)$. To compute the mean and variance of $B(t|\theta)$, we integrate (5.4) - (5.5) with respect to $p(h|\theta)dh$ where $p(h|\theta)$ is given by (2.4):

Theorem 6.1. For $t < \theta$,

$$E[B(t|\theta)] = \int_0^\infty E[B(t)|\theta, h]p(h|\theta)dh = \sqrt{\frac{\pi\theta}{2}} - \int_0^\infty M_1(1 - \frac{t}{\theta}, \frac{h}{\sqrt{\theta}}) \frac{h}{\sqrt{\theta}} e^{-\frac{h^2}{2\theta}} dh \quad (6.1)$$

$$= \sqrt{\frac{\pi\theta}{2}} - \sqrt{\theta}G_{11}(s) = \sqrt{\frac{\pi\theta}{2}} - \sqrt{\frac{2\theta}{\pi}} \left[\tan^{-1}(\sqrt{\frac{s}{1-s}}) + \sqrt{s(1-s)} \right] , \quad (6.2)$$

where $s \equiv 1 - \frac{t}{\theta}$ and G_{11} is given in (5.6). For $t > \theta$, the expectation becomes

$$E[B(t|\theta)] = \sqrt{\frac{\pi\theta}{2}} - \sqrt{\frac{2(1-\theta)}{\pi}} \left[\tan^{-1}(\sqrt{\frac{s}{1-s}}) + \sqrt{s(1-s)} \right] \quad \text{for } t \geq \theta \quad (6.3)$$

where $s \equiv \frac{t-\theta}{1-\theta}$.

For the variance, we first evaluate $E[B^2(t|\theta)]$ and then subtract off $E[B(t|\theta)]^2$.

$$E[B^2(t|\theta)] = 2\theta - 4\theta\sqrt{s} + \theta[3s - s^2] \quad \text{for } t \leq \theta \quad (6.4)$$

For $t \geq \theta$, the variance simplifies:

$$\text{Var}[B(t|\theta)] = \text{Var}[h|\theta] + (1 - \theta) [3s - s^2 - G_{11}(s)^2] , \quad (6.5)$$

where $\text{Var}[h|\theta] = (2 - \pi/2)\theta$.

Proof: We use the integrals in (9.13) - (9.15) of the Appendix A and set $s = 1 - t/\theta$. To prove (6.4), note

$$E[B^2(t|\theta)] = \int_0^\infty E[B^2(t)|\theta, h]p(h|\theta)dh = \int_0^\infty [\theta x^2 - 2\theta x M_1(s, x) + M_2(s, x)] x e^{-\frac{x^2}{2}} dx \quad (6.6)$$

and insert the expression in (9.17) - (9.18).

Our expression matches the zero dimensional results derived in the second section, $E[h|\theta] = \sqrt{\pi\theta/2}$, $Var[h|\theta] = (2 - \pi/2)\theta$.

Let $g(t, \theta) = E[B(t)|\arg\max B = \theta]$. Figure 1 plots $g(t, \theta)$ for ten quantile values of the bins in θ ranging from the second smallest bin to the second largest bin. Unsurprisingly, the $g(t, \theta)$ is maximized at $t = \theta$ for fixed θ . The curves look monotone for θ very near 0 or 1, but this is a graph and simulation resolution effect. Even at $n\text{bins} = 160$, there is still a small amount of artificial broadening of the peak due to averaging $g(t, \theta)$ over the bin. Using the density (2.6), we calculate $E[h|\theta] = \sqrt{\pi\theta/2}$.

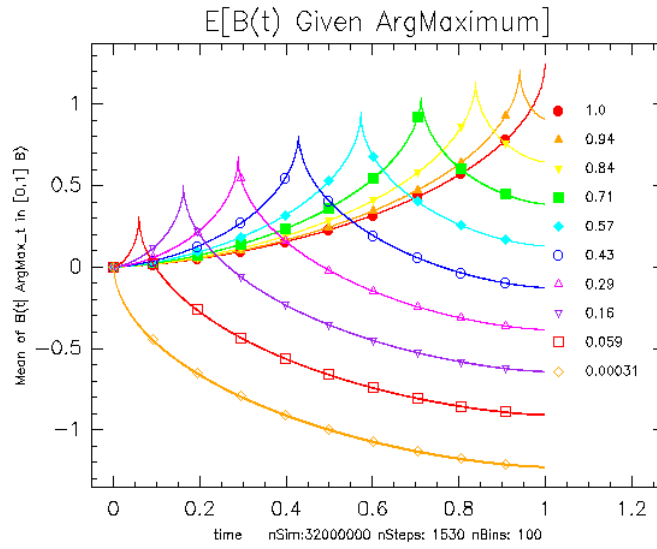


Figure 1: Expectation of $B(t)$ given $\theta \equiv \arg\max\{B(t)\}$ for various values of θ . Each color has two curves, a theoretical curve from Theorem 6.1 and the mean value of the simulation for the given parameter bin. To compute the simulation expectation, we use an ensemble of 32,000,000 realizations computed with 1500 steps and bin the results into 100 bins in θ space. The values of θ for each curve are given in the legend.

Figure 2 plots the variance, $var(t, \theta) = Var[B(t)|\arg\max B = \theta]$. For small values of θ , $var(t, \theta)$ grows linearly for most time, then it accelerates as θ approaches 1. For larger values of θ , it appears that $\frac{\partial var(t, \theta)}{\partial t}$ is nearly a constant for t near zero. The growth rate decelerates in time and this deceleration occurs earlier for smaller θ . From (2.10), $Var[B(1)|\theta] = 2(1 - \pi/4) \approx 0.4292$.

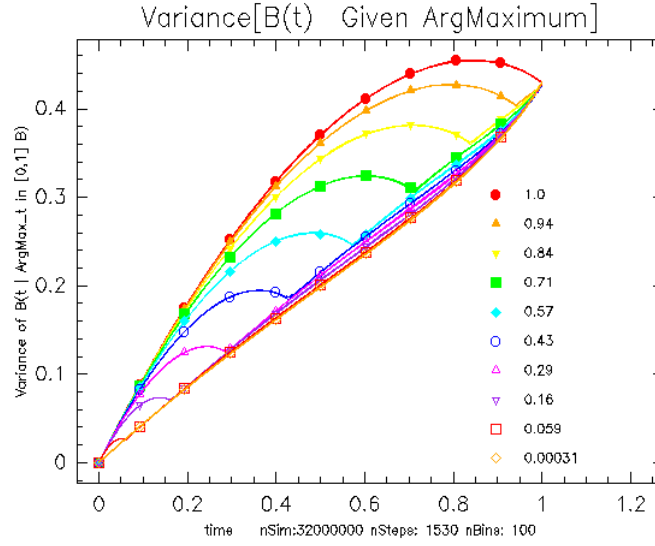


Figure 2: Variance of $B(t)$ given $\theta \equiv \operatorname{argmax}\{B(t)\}$ for various values of θ . When θ is small, the variance grows roughly linearly in time. For larger values of θ , the variance grows faster initially and then converges to the linear value.

7 Overview of Simulation Results

We generate a large number of Brownian paths, bin the paths in $(close, \max, \operatorname{argmax})$ space and calculate the mean and variance for each time and bin. We order the coordinates of phase space, (q_1, q_2, q_3) , so that $q_1 = B(1)$, $q_2 = \max_{0 \leq t \leq 1} B(t)$ and $q_3 = \operatorname{argmax}_{0 \leq t \leq 1} B(t)$. To see $E[B(t)|givens]$ and $Var[B(t)|givens]$, we simulate 10 to 36 million Brownian motions. A detailed description of the simulation method may be found in Appendix B and [17]. We display simulations using 1500-1850 time steps for each realization.

For each bin, we compute the expectation and variance using (4.7) - (4.11). In Appendices C, D and E, we present a number of figures displaying and explaining the behavior of $E[B(t)|c, \theta, h]$ and $Var[B(t)|c, \theta, h]$ as t, c, θ, h vary.

We evaluate the discrepancy/mean square error (MSE) between the theoretical formulae and our simulations. For each bin in parameter space, we compare the difference between (4.7) and the average of the curves in the bin. We then compute the mean squared error averaged over time:

$$MSE(c, \theta, h) = \int_0^1 \left(E[B(t)|c, \theta, h] - Avg_j[\tilde{B}_j(t|c, \theta, h)] \right)^2 dt \quad (7.1)$$

where \tilde{B}_j is the j curve in the bin and Avg_j is the average over all of the paths in the given bin in parameter space. We then sort the bins from worst to best MSE. Not surprisingly the worst fitting bins often occur where the bins are the largest and the bias error, from having curves with slightly different parameters, is the largest.

Overall, the concatenated meander expectation fits the simulation expectation very well. To further illustrate this, we overlay all four sets of curves on the same plot. Figure 3 plots the curves that correspond to the worst 5%, 2%, 1% and 0.2% difference between the simulation conditional mean and (4.7) - (4.9). There are $120^3 \geq 1.7$ million bins to compare. The curves overstruck by symbols are the simulation curves. The analytic formula curves have the same color but no symbol.

We conclude with a comparison of the variance of the simulation with the concatenated meander in (4.10) - (4.11). Figure 4 plots the curves that correspond to the worst 5%, 2%, 1% and 0.2% difference

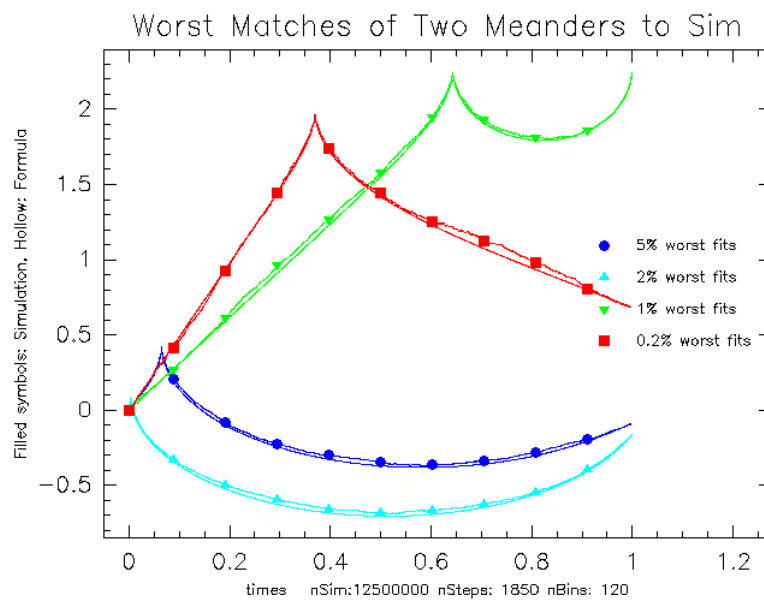


Figure 3: Comparison of Formula and Simulation: Each color has two curves, a theoretical curve from Theorem 4.3 and the mean value of the simulation for the given parameter bin. The curves overstruck by symbols are the simulation curves. The analytic formula curves have the same color but no symbol.

Blue: 5% worst MSE Mean:0.00039 at close:-0.0891, high:0.431, argmax:0.065

Cyan: 2% worst MSE Mean:0.000507 at close:-0.166, high:0.101, argmax:0.00374

Green: 1% worst MSE Mean:0.000608 at close:2.246, high:2.27, argmax:0.643

Red: 0.2% worst MSE Mean:0.00091 at close:0.682, high:1.991, argmax:0.37

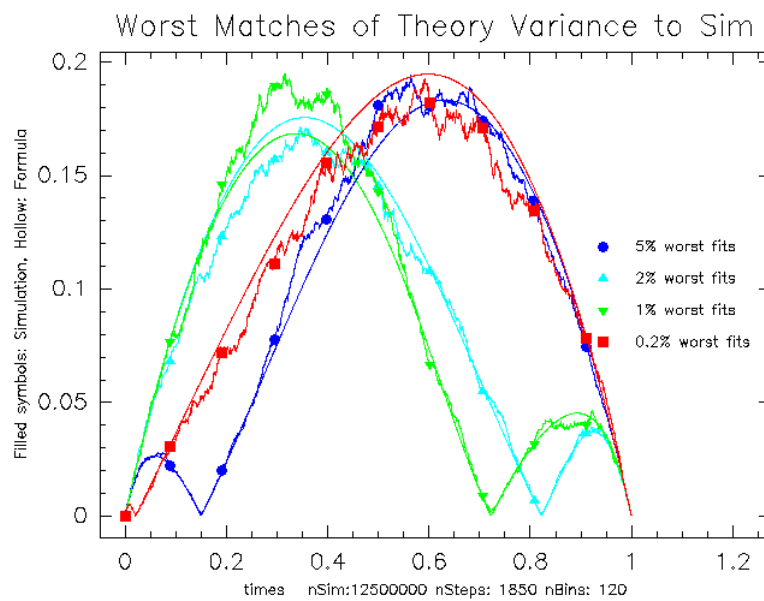


Figure 4: Comparison of Meander Variance Formula and Simulation: Each color has two curves, a theoretical variance and the variance of the simulation for the given parameter bin.

The symbols are on the curve from the simulation.

Blue: 5% worst MSE Var:.000054 at close:-1.743, high:0.55, argmax:0.15

Cyan:2% worst MSE Var:.0000775 at close:1.246, high:2.177, argmax:0.822

Green:1% worst MSE Var:.0000981 at close:2.531, high:3.164, argmax:0.723

Red:0.2% worst MSE Var:0.000159 at close:-1.437, high:0.461, argmax:0.0208

between the simulation conditional variance and (4.10) - (4.11). In Appendix C, we display the analogous plots for $E[B(t|\theta, h)]$. As expected, averaging over values of c reduces the noise in the simulations and reduces the discrepancy.

8 Summary

We have investigated the distribution, expectation and variance of Brownian motion conditional on the values of its maximum and its location as well as its final value. We give formulae for the mean and variance of a Brownian meander. Using the Williams construction, we evaluate the expectation and variance, $E[B(t)|c, \theta, h]$ and $Var[B(t)|c, \theta, h]$. To analyze $B(t|\theta, h)$ and $B(t|\theta)$, we integrate the distribution and moments with respect to the close, c , and then with respect to the maximum, h . Similar but more complex formulae can be calculated for $B(t|\theta, c)$. Our simulations show good agreements with the analytic expressions. Many interesting features are displayed in the figures of the mean and variance. Figure 5 displays the ensemble average of the variance of $B(t|givens)$. For example,

$$V(t|givens = (c, \theta, h)) \equiv \int Var[B(t|c, \theta, h)] dp(c, \theta, h) . \quad (8.1)$$

We compare the ensemble averages of $Var[B(t|argmax)]$ with $Var[B(t|close)], Var[B(t|close, argmax)]$ and $Var[B(t|close, argmax, high)]$. In all case, we compute the variance for each value of the givens separately and then average over the distribution of the givens. From Figure 5, we see that argmax

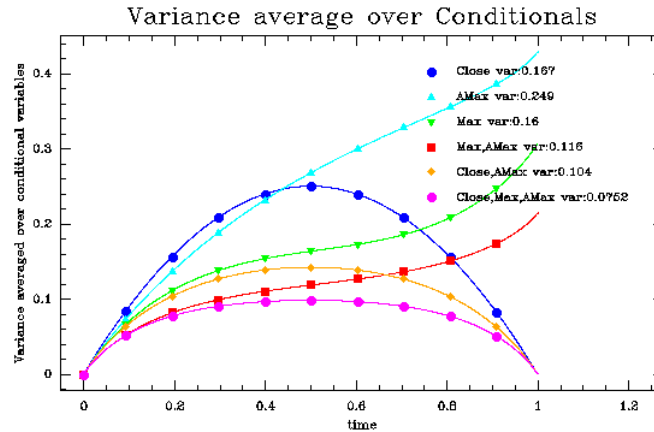


Figure 5: Comparison of $Var[B(t|close)], Var[B(t|close)]$, versus $Var[B(t|close, argmax)]$ versus $Var[B(t|close, argmax, high)]$. These curves are the ensemble average over all of the simulations.

is a much less valuable statistic than either the *close* or *max*. The statistics, $(close, argmax)$, are more valuable than the pair of statistics $(max, argmax)$. If the final value (*close*) is known, the variance is symmetric in time. Otherwise, the variance increases in time.

We conclude by merging our results with those in [17]. To measure how accurately we can estimate $B(t|\theta, h, c)$, we consider the time integral of the conditional variance averaged over the given variables: $\int_0^1 Var[B(t|c, \theta, h)] dt dp(c, \theta, h)$. If only the final value, c , is specified, the value of the integral is $1/6$. Table 1 presents the corresponding values for our simulations in this paper. This shows that the statistics triple $(Close, High, Low)$ is more valuable than the triple $(Close, High, ArgMax)$. In all cases, adding addition information such as the value of the high and/or its location significantly reduces the time averaged variance in comparison with that of the Brownian bridge (i.e only using the final value of $B(t = 1)$).

In our sister article [17], we show using the high, low and close substantially improves the estimation of the log return of the SP500 over using just the close. We can reproduce this calculation/application

Givens	Var	Var*6
Start point only	1/2	3
Close	1/6	1
High	0.1602	.9612
ArgMax	.2487	1.492
Close, High	0.0990	.5938
Close, ArgMax	0.1037	.6222
Argmax, High	0.11585	0.6951
Close, High, ArgMax	0.07535	.4521
Close, High, Low	0.0701	.4206

Table 1: Expected time average variance reduction. We multiply the variance by 6 in the third column to compare with knowing only the final value, c .

in this article, but it will be artificial. The reason is that the location of the maximum is seldom if ever used to parameterize a stochastic process. In contrast, chartist analysis in finance heavily uses the values of the high and low. Note that Table 1 shows that using the value of the maximum is better than using the value of arg maximum.

9 Appendix A: Meander Moments

We now compute moments

$$M_k(s, t, c) = \int_0^\infty x^k P(B^{me}(s) = x | B^{me}(t) = c) dx \quad (9.1)$$

$$= \int_0^\infty (\phi_{t-s}(c-x) - \phi_{t-s}(c+x)) \frac{x^k t^{3/2}}{cs^{3/2}} \exp(-x^2/2s) \exp(c^2/2t) dx \quad (9.2)$$

$$= \frac{t^{3/2}}{cs^{3/2}} \frac{2}{\sqrt{2\pi\tau}} \exp(-c^2/2h) \exp(c^2/2t) \int_0^\infty x^k \exp(-ax^2) \sinh(bx) dx, \quad (9.3)$$

where $\tau \equiv t-s$, $a \equiv \frac{1}{2\tau} + \frac{1}{2s} = \frac{t}{2s(t-s)}$ and $b \equiv \frac{c}{t-s}$. Note $M_0(s, t, c) = 1$:

$$M_0(s, t, c) = \frac{t^{3/2}}{cs^{3/2}} \frac{1}{\sqrt{2\pi\tau}} \exp(-c^2/2h) \exp(c^2/2t) \frac{\sqrt{\pi}b}{2\sqrt{a^3}} e^{\frac{b^2}{4a}} = 1. \quad (9.4)$$

Here we use $b^2/4a = c^2s/2t(t-s)$ and $\frac{1}{2h} - \frac{1}{2t} = \frac{s}{2t(t-s)}$ to show that the exponential terms cancel. The first moment of the meander satisfies

$$M_1(s, t, c) = \frac{t^{3/2}}{cs^{3/2}} \frac{1}{\sqrt{2\pi\tau}} \exp(-c^2/2h) \exp(c^2/2t) \left[\frac{\sqrt{\pi}[2a+b^2]e^{\frac{b^2}{4a}} \operatorname{erf}(\frac{b}{2\sqrt{a}})}{4a^{2.5}} + \frac{b}{2a^2} \right] \quad (9.5)$$

$$= \frac{[t-s+sc^2/t] \operatorname{erf}(\frac{c\sqrt{s}}{\sqrt{2t(t-s)}})}{c} + \frac{\sqrt{2s(t-s)}}{\sqrt{\pi t}} \exp(-sc^2/2t(t-s)). \quad (9.6)$$

Similarly, the second moment of the meander satisfies

$$M_2(s, t, c) = \frac{t^{3/2}}{cs^{3/2}} \frac{1}{\sqrt{2\pi\tau}} \exp(-c^2/2h) \exp(c^2/2t) \frac{\sqrt{\pi}b(6a+b^2)e^{\frac{b^2}{4a}}}{8a^{7/2}} = \quad (9.7)$$

$$= \frac{t^{3/2}}{cs^{3/2}} \frac{1}{\sqrt{2(t-s)}} \frac{b(6a+b^2)}{8a^{7/2}} = \frac{t^{3/2}}{s^{3/2}} \frac{1}{\sqrt{2(t-s)^{1.5}}} \frac{(1.5+b^2/4a)}{2a^{5/2}} \quad (9.8)$$

$$= (3+c^2s/t(t-s)) \left(\frac{s(t-s)}{t} \right) = \frac{3s(t-s)}{t} + c^2s^2/t^2. \quad (9.9)$$

The integrations follow from

$$\int_0^\infty x \exp(-ax^2) \sinh(bx) dx = \frac{\sqrt{\pi}b}{4\sqrt{a^3}} e^{\frac{b^2}{4a}} \quad (9.10)$$

$$\int_0^\infty x^2 \exp(-ax^2) \sinh(bx) dx = \frac{\sqrt{\pi}[2a + b^2]e^{\frac{b^2}{4a}} \operatorname{erf}(\frac{b}{2\sqrt{a}})}{8a^{2.5}} + \frac{b}{4a^2} \quad (9.11)$$

$$\int_0^\infty x^3 \exp(-ax^2) \sinh(bx) dx = \frac{\sqrt{\pi}b(6a + b^2)e^{\frac{b^2}{4a}}}{16a^{7/2}} . \quad (9.12)$$

For Section 5, we need the following integral:

$$\int_0^\infty x M_1(s, x) e^{-\frac{x^2}{2}} dx = \int_0^\infty (1 - s + sx^2) e^{-\frac{x^2}{2}} \operatorname{erf}(x\sqrt{\frac{\kappa}{2}}) + \sqrt{\frac{2}{\pi}} \sigma(s) x e^{-\frac{x^2}{2(1-s)}} dx \quad (9.13)$$

$$= \sqrt{\frac{2}{\pi}} \left[\tan^{-1}(\sqrt{\kappa}) + s \frac{\sqrt{\kappa}}{\kappa + 1} + \sqrt{s(1-s)^3} \right] \quad (9.14)$$

$$= G_{11}(s) \equiv \sqrt{\frac{2}{\pi}} \left[\tan^{-1}\left(\sqrt{\frac{s}{1-s}}\right) + \sqrt{s(1-s)} \right] , \quad (9.15)$$

where $\kappa = s/(1-s)$ and $\sigma(s) \equiv \sqrt{s(1-s)}$. We use the identities: $\int_0^\infty \operatorname{erf}(\frac{ax}{\sqrt{2}}) \exp(-\frac{x^2}{2}) dx = \sqrt{\frac{2}{\pi}} \tan^{-1}(a)$ and $\sqrt{\frac{\pi}{2}} \int_0^\infty x^2 \operatorname{erf}(\frac{ax}{\sqrt{2}}) \exp(-\frac{x^2}{2}) dx = \frac{a}{a^2+1} + \tan^{-1}(a)$. To evaluate the variance, we need

$$\int_0^\infty M_2(s, x, 1) x e^{-\frac{x^2}{2}} dx = \int_0^\infty (3s(1-s) + x^2 s^2) x e^{-\frac{x^2}{2}} dx = [3s(1-s) + 2s^2] = [3s - s^2] . \quad (9.16)$$

To evaluate $E[B^2(t|\theta)]$ in (6.4), note

$$\int_0^\infty x^2 M_1(s, x) e^{-\frac{x^2}{2}} dx = \int_0^\infty (1 - s + sx^2) x e^{-\frac{x^2}{2}} \operatorname{erf}(x\sqrt{\frac{\kappa}{2}}) + \sqrt{\frac{2}{\pi}} \sigma(s) x^2 e^{-\frac{x^2}{2(1-s)}} dx \quad (9.17)$$

$$= (1-s) \frac{\sqrt{\kappa}}{\sqrt{1+\kappa}} + s\sqrt{\kappa} \frac{2\kappa+3}{(1+\kappa)^{3/2}} + \sigma(s) * (1-s)^{3/2} = 2\sqrt{s} . \quad (9.18)$$

We used the identities: $\int_0^\infty x \operatorname{erf}(\frac{ax}{\sqrt{2}}) \exp(-\frac{x^2}{2}) dx = \frac{a}{\sqrt{1+a^2}}$ and $\int_0^\infty x^3 \operatorname{erf}(\frac{ax}{\sqrt{2}}) \exp(-\frac{x^2}{2}) dx = a(2a^2+3)/(a^2+1)^{3/2}$.

10 Appendix B: Details of Brownian Simulations

In the simulation, we generate about 17 million Brownian paths. We then bin the paths in a “grid” of bins in $(close, \theta, high)$ space. We use quantile-like coordinates in the (q_1, q_2, q_3) parameterization. In the first phase space direction, $q_1 = c$, compute bin boundaries so that the number of curves are roughly equal in each bin. For each one dimensional bin, compute bin boundaries in the second coordinate direction, h , so that the number of bins is roughly equal. Finally, for each of the two dimensional bins, compute bins in the third direction, θ . Often, we choose a grid in c to correspond to quantiles of the normal distribution. (We center the c values to be the midpoints of the c grid.) The advantage of this approach is that the number of curves in each simulations is approximately the same. The disadvantage of this approach is that a convergence analysis is hard because the coordinates vary from simulation to simulation and halving the coordinate distance cannot be done in this adaptive gridding.

Given an ensemble of Brownian paths, $\{B_i(t)\}$, we can create an equivalent ensemble of Brownian paths, $\{B_i(t, c)\}$, with right endpoint c , using the formula: $B_i(t, c) \equiv B_i(t) - (B_i(t=1) - c)t$. In our case, we transform the original 10 to 36 million Brownian paths for each value of c , calculate the maximum, h , and arg-maximum, θ , of $B_i(t, c)$. We then bin the paths into an $nbins \times nbins$ grid in (θ, h) space

based on the quantiles of the (θ, h) . A typical values of $n\text{bins}$ are from 80 to 120. For each bin in the $(\text{close}, \theta, h)$ grid, we calculate the mean and variance for each time and bin.

To describe these simulations, we call $n\text{Steps}$, the number of timesteps in the any one path simulation and $n\text{Sim}$ is the number of Brownian paths that we compute in the simulation before shifting the paths to have final value c .

The values of argmax occur only on the time grid and this makes the quantile buckets discrete. To regularize the discreteness of argmax , we use a quadratic interpolation of argmax , i.e. for a given realization of $B(t)$ on a discrete path, we find the argmax on the grid, $\{t_i\}$. We then use quadratic interpolation of $B(t)$ on $B(t_{i-1})$, $B(t_i)$ and $B(t_{i+1})$ to find a better approximation to the continuous time value of argmax . A more accurate calculation is to use the expectation of the argmax conditional on the three point values $B(t_{i-1})$, $B(t_i)$, $B(t_{i+1})$ where the discrete minimum occurs at $B(t_i)$ [1].

11 Appendix C: Plots of Mean and Variance Given High and Argmax

Figure 6 displays the expectation of $B(t|\theta = .507, h)$ for various values of the high. The maximum is at θ and decays as $t \rightarrow 1$. The values of the high are spaced accordingly: For the given values of θ , we display the the values of the high corresponding to the second smallest and second largest bins and eight equi-spaced values of h . Figure 6 displays the expectation of $B(t|\theta = .507, h)$ for various

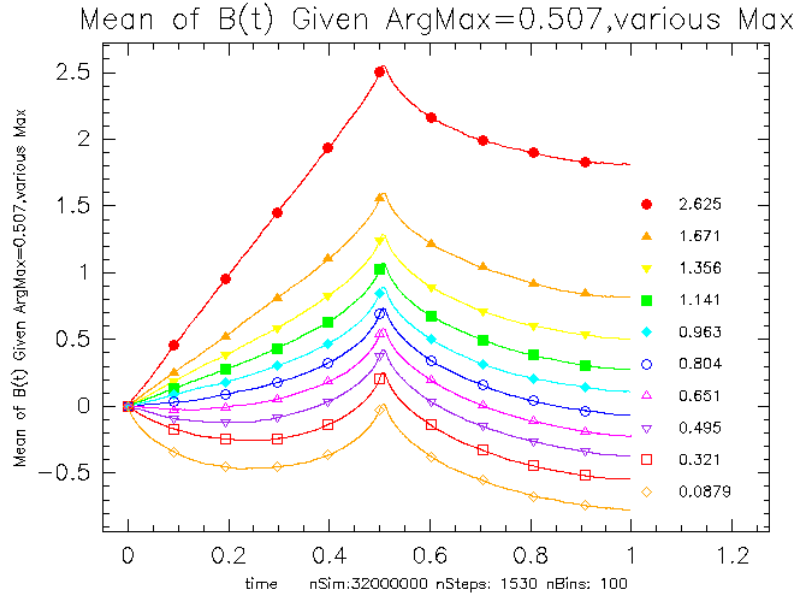


Figure 6: $E[B(t|\text{argmax} = 0.507, \text{various high})]$. The h values are spaced at roughly quantile values of $k/9$ given. The values of the high are given in the legend.

values of the high and Figure 7 displays the analogous variance. The variance should be zero at θ however the curve for the largest value of h does not satisfy this as the discrete binning effect has curves corresponding to a variety of different θ and the mean of the curves in this edge bin is not equal to the average of the expectations but simply the average of the realizations. We see that the variance is roughly parabolic for $t \in [0, \theta]$ and then grows beyond θ . Figures 8-10 display the other cross sections for different values of θ with a fixed maximum, h . Plotting the variance for these cross sections again shows a rounded shape for $t \leq \theta$ and a roughly linear growth rate for $t \geq \theta$. For $t < \theta$, the curves rise more rapidly near $t = 0$ than they decrease near $t \approx \theta$. The local maximum of the variance occurs before $t = \theta/2$.

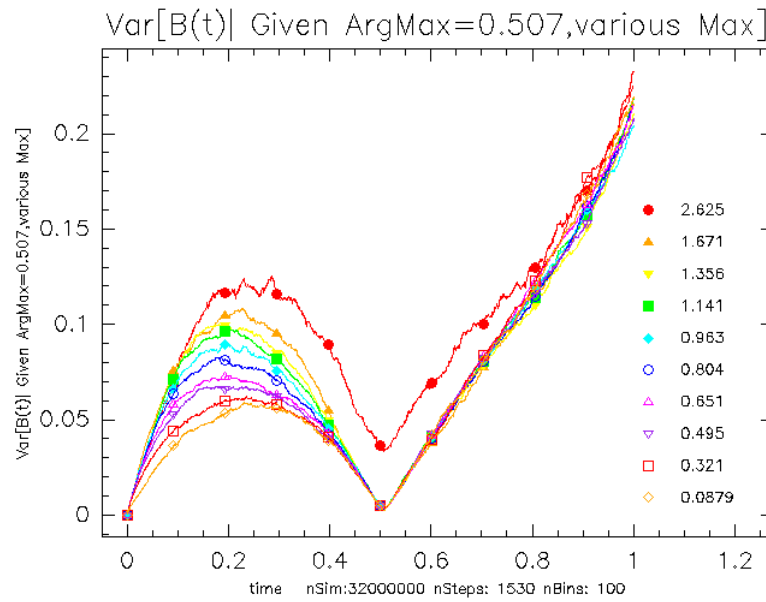


Figure 7: $\text{Var}[B(t)|\text{argmax} = 0.507, \text{various high}]$ where the values of max as given in the legend.

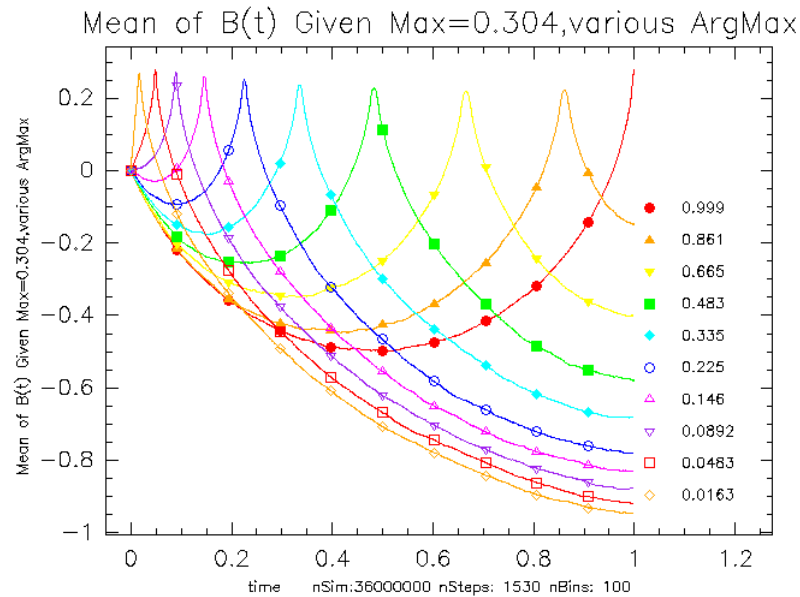


Figure 8: $E[B(t)|\text{max} = 0.304, \text{argmax}]$. Here .304 is roughly the .2 quantile of the high. The θ values are spaced at roughly quantile values of $k/9$ given, h .

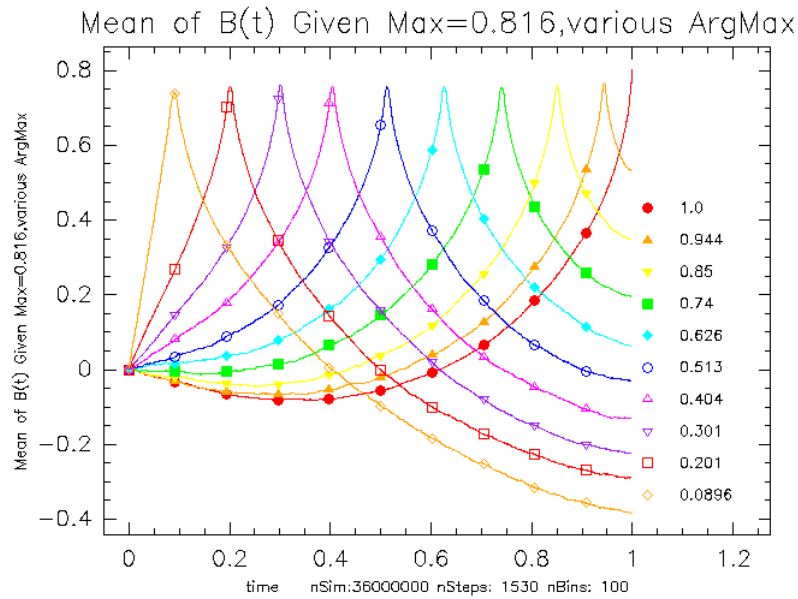


Figure 9: $E[B(t)|\text{max} = 0.816, \text{various argmax}]$. Here .816 is roughly the median of the high. The θ values are spaced at roughly quantile values of $k/9$ given, h .

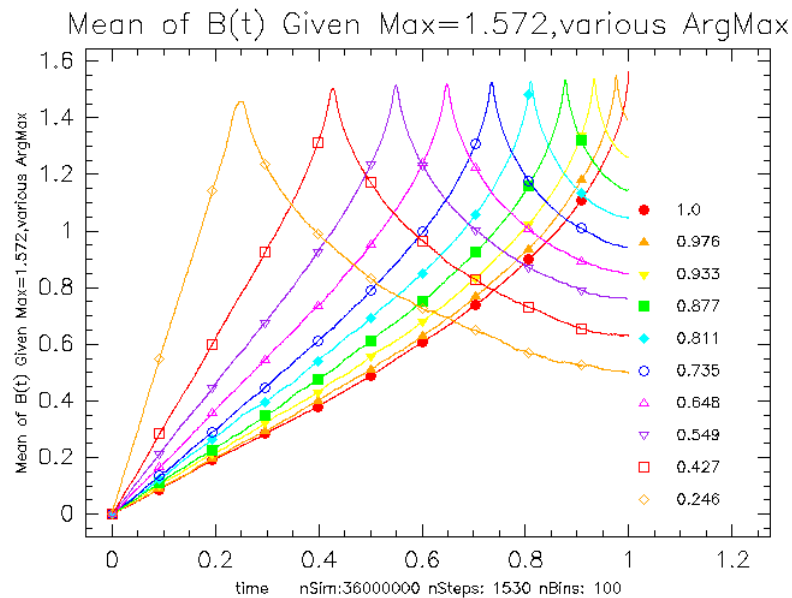


Figure 10: $E[B(t)|\text{max} = 1.572, \text{various argmax}]$. Here 1.572 is roughly the .2 quantile of the high. The θ values are spaced at roughly quantile values of $k/9$ given, h .

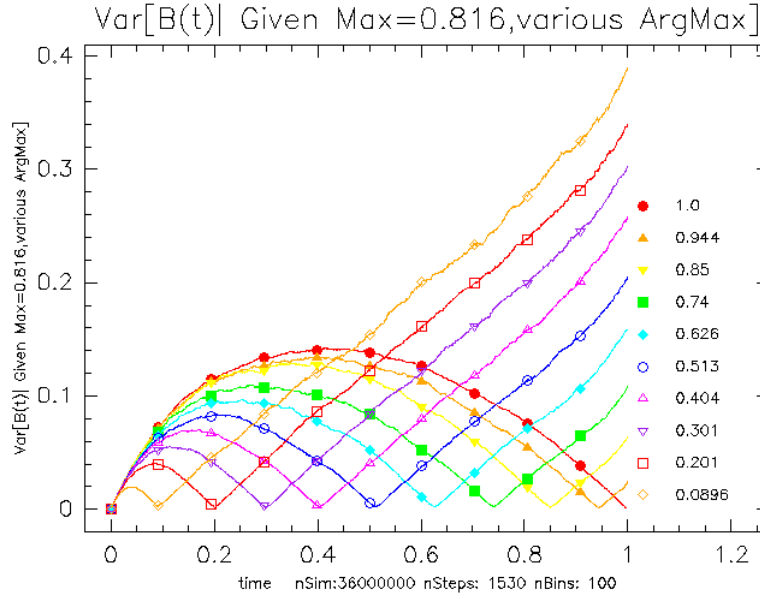
Figure 11: $Var[B(t)|max = 0.816, various \text{ argmax}]$

Figure 12 and Figure 13 compare our simulations with the analytic expressions in (5.4) - (5.5). In the simulation, we use $120^3 \approx 1.7M$ bins for binning the values of $(close, \theta, high)$. For each bin, we compute the expectation and variance using (4.7) - (4.11), and then evaluate the time average of the mean square error. We then sort the bins from worst to best MSE. Not surprisingly the worst fitting bins often occur where the bins are the largest and the bias error, from having curves with slightly different parameters, is the largest. Figure 12 plots the curves that correspond to the worst 5%, 2%, 1% and 0.2%. Since we evaluate the worst fitting curves for the expectation and variance separately, the parameters for the worst fits for the expectation differ from the corresponding parameters for the variance plots. The curves overstruck by symbols are the simulation curves. The analytic formula curves have the same color but no symbol. Overall, the concatenated meander expectation fits the simulation expectation very well.

The MSE in Figure 12 is less than the MSE in Figure 3. As expected, averaging over values of c reduces the noise in the simulations and reduces the discrepancy.

We conclude with a comparison of the variance of the simulation with the concatenated meander in (4.10) - (4.11).

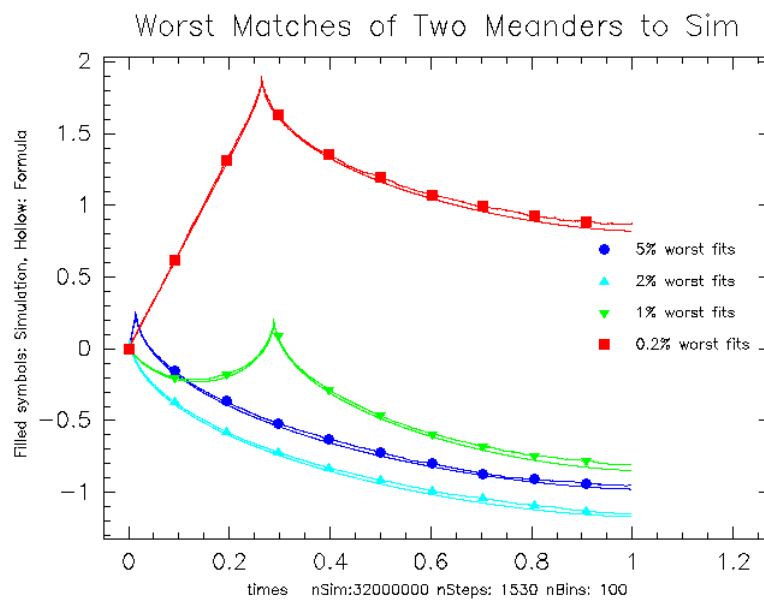


Figure 12: Comparison of Formula and Simulation:

Blue: 5% worst MSE Mean:0.000433 high:0.267, argmax:0.0142

Cyan: 2% worst MSE Mean:0.000554 high:0.0825, argmax:0.00224

Green: 1% worst MSE Mean:0.000639 high:0.21, argmax:0.289

Red: 0.2% worst MSE Mean:0.000826 high:1.897, argmax:0.265

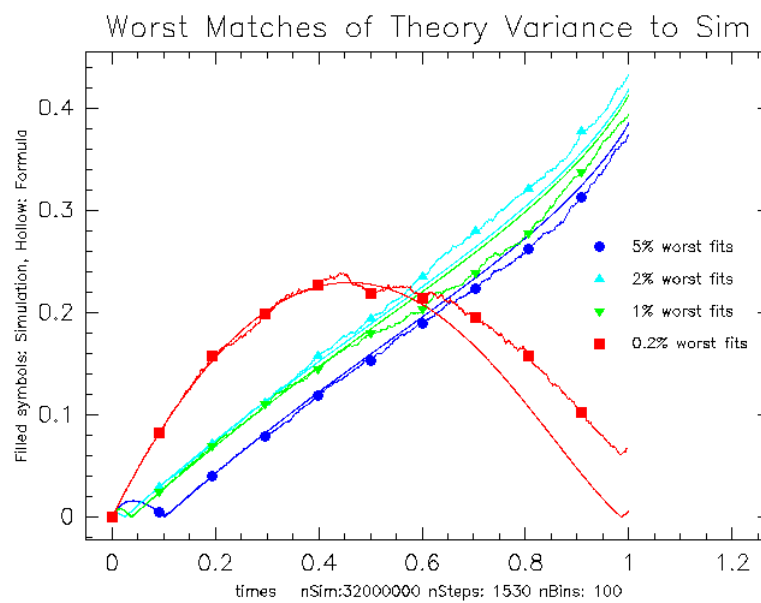


Figure 13: Comparison of Meander Variance Formula and Simulation:

Blue: 5% worst MSE Var:0.0000541, high:0.329, argmax:0.102

Cyan:2% worst MSE Var:0.0000943, high:0.127, argmax:0.0247

Green:1% worst MSE Var:0.000143, high:0.46, argmax:0.0376

Red:0.2% worst MSE Var:0.000857, high:3.658, argmax:0.986

12 Appendix D: Time Dependent Behavior of Moments Given Close, Argmax, High

The figures in this section are from our simulation without the corresponding analytic calculations.

12.1 Expectation Given Close, Argmax, High

The next five figures display $E[B(t)|close, argmax, high]$. Each figure fixes values of the close and $\theta = \argmax\{B(t)\}$. The values of the close are roughly $\{-1, 0, +1\}$. In this section, we use 12.5 million realizations with 1850 time steps. We divide the parameter space into 120 bins in parameter direction. For each realization, we shift all of the sample paths to have the same close. For each close, the 12.5M realizations are binned into the 120^2 bins. Thus the empirical mean and variance are noisier than in Section 13 where the realizations were divided into only 120 bins. We plot both the empirical curves from our simulation and the theoretical values from (4.7) - (4.11) in the same color. The curves overstruck by symbols are the simulation curves. The analytic formula curves have the same color but no symbol. The smooth curves are the theoretical ones while the noisy curves are the simulated ones.

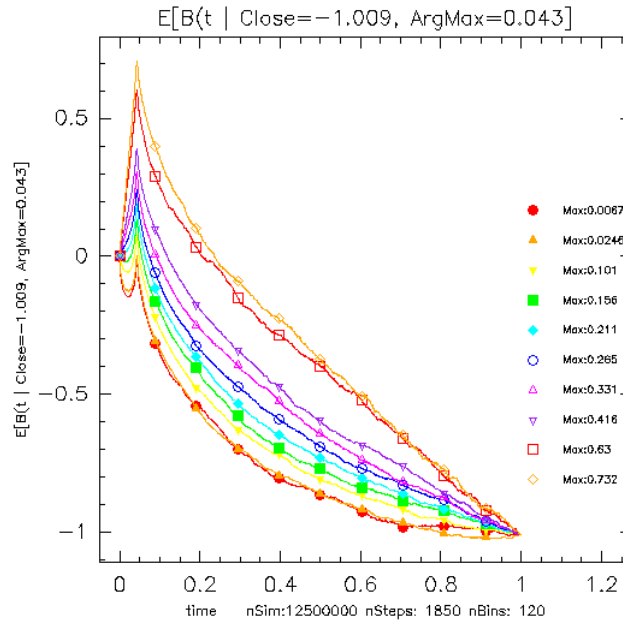


Figure 14: $E[B(t)|close, argmax, high]$ where $close = -1.009$ and $argmax = 0.043$. Each curve is a given value of $high = \max\{B(t)\}$.

For $close = 0$, we have the symmetry: $E[B(t)|c = 0, h, \theta] = E[B(t)|c = 0, h, 1 - \theta]$. Rather than plot figures for $close = 1$, we again the reflection symmetry: $E[B(t) - c, \theta, h] = E[B(1 - t|c, 1 - \theta, h + c)] - c$.

Brownian Motion Moments

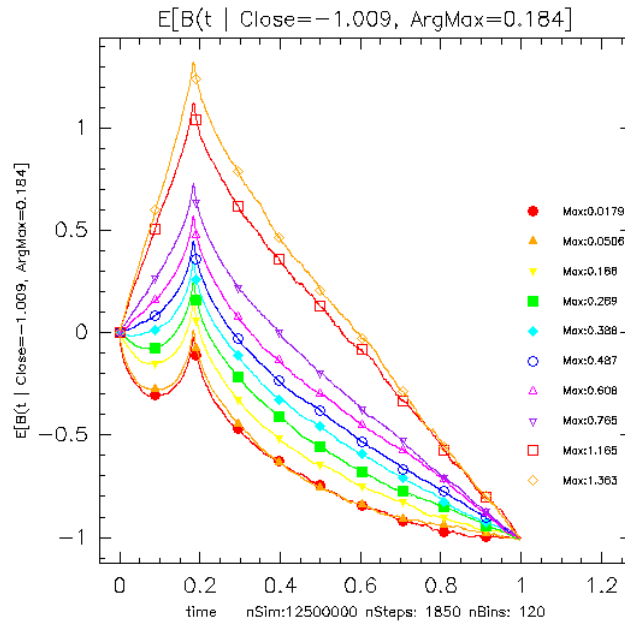


Figure 15: $E[B(t|close, argmax, high)]$ where $close = -1.009$ and $\theta = 0.184$. The values of the high are given in the legend. For larger values of the high, the $E[B(t)]$ is approximately piecewise linear with a maximum at θ .

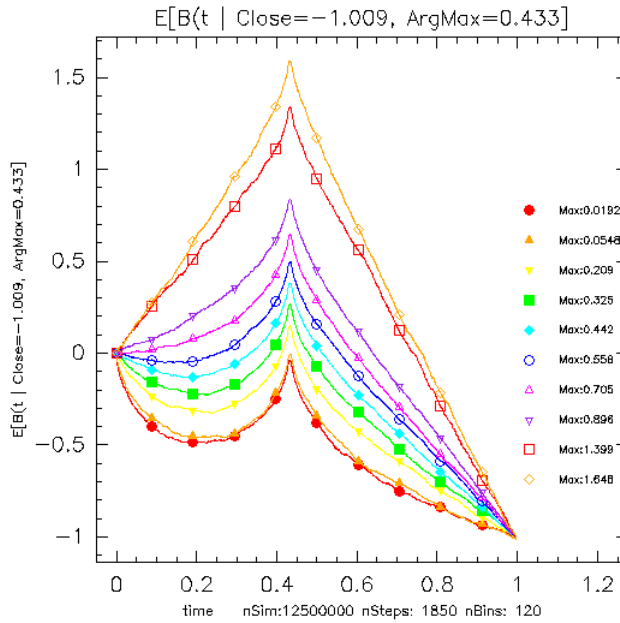


Figure 16: $E[B(t|close, argmax, high)]$ where $close = -1.009$ and $argMax = 0.433$. Each curve is a given value of $high = \max\{B(t)\}$ as denoted in the legend.

Brownian Motion Moments

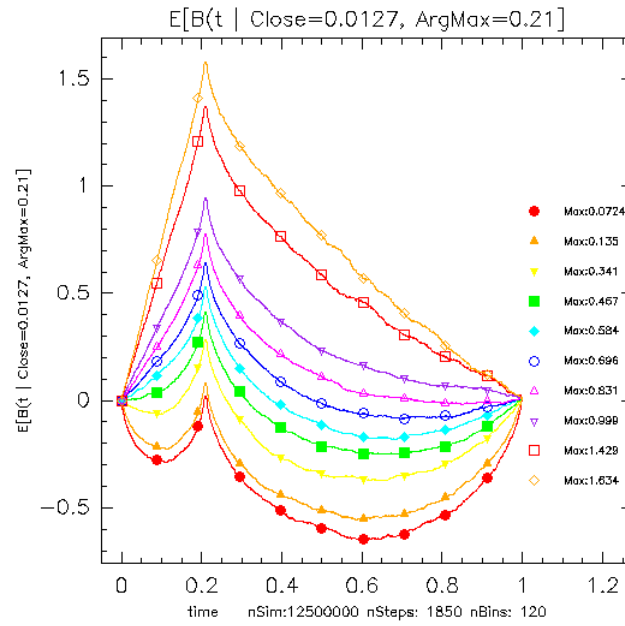


Figure 17: $E[B(t)|close, high, \text{argmax}]$ where $close=0.0127$ and $\theta=0.21$. For larger values of the high, the $E[B(t)]$ grows approximately linearly until θ and then decays back to its final value.

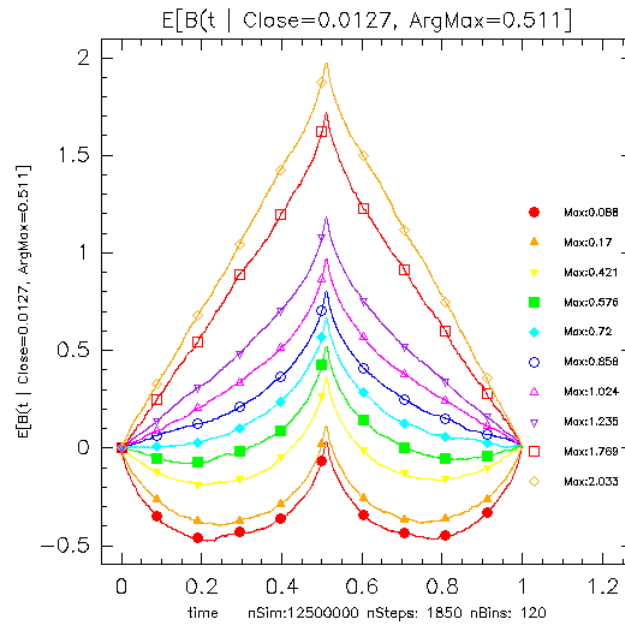


Figure 18: $E[B(t)|close, \text{argmax}, high]$ where $close=0.0127$, $\theta=0.511$, and $\max B$ is given in the legend. . Since the close is nearly zero and θ is nearly 0.5, the curves are nearly symmetric in time.

12.2 Variance Given Close, Argmax, High

We now display $\text{Var}[B(t)|\text{close}, \text{argmax}, \text{high}]$. Each figure fixes values of the close and $\theta = \text{argmax}\{B(t)\}$. The curves overstruck by symbols are the simulation curves. The analytic formula curves have the same color but no symbol. The simulation curves have a larger value because they include the bias^2 term.

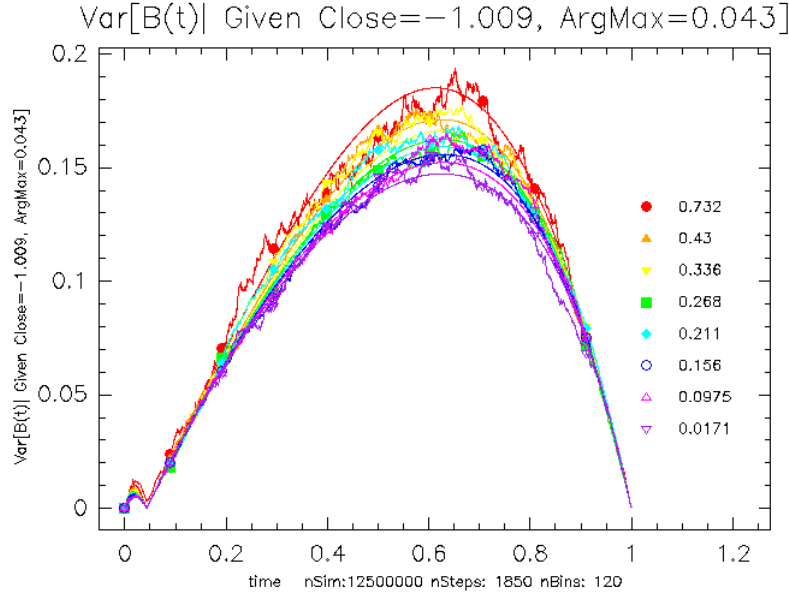


Figure 19: $\text{Var}[B(t)|\text{close}, \text{argmax}, \text{high}]$ where $\text{close} = -1.009$ and $\text{argMax} = 0.043$. The value of θ is small, therefore the variance has a local minimum at θ and then increases. The variance profile appears especially flat near its maximum.

Rather than plot figures for $\text{close} = 1$, we use the reflection symmetry: $\text{Var}[B(t)|-c, \theta, h] = \text{Var}[B(1-t)|c, 1-\theta, h+c]$. For $\text{close} = 0$, we have the symmetry: $\text{Var}[B(t)|c = 0, \theta, h] = \text{Var}[B(t)|c = 0, 1-\theta, h]$

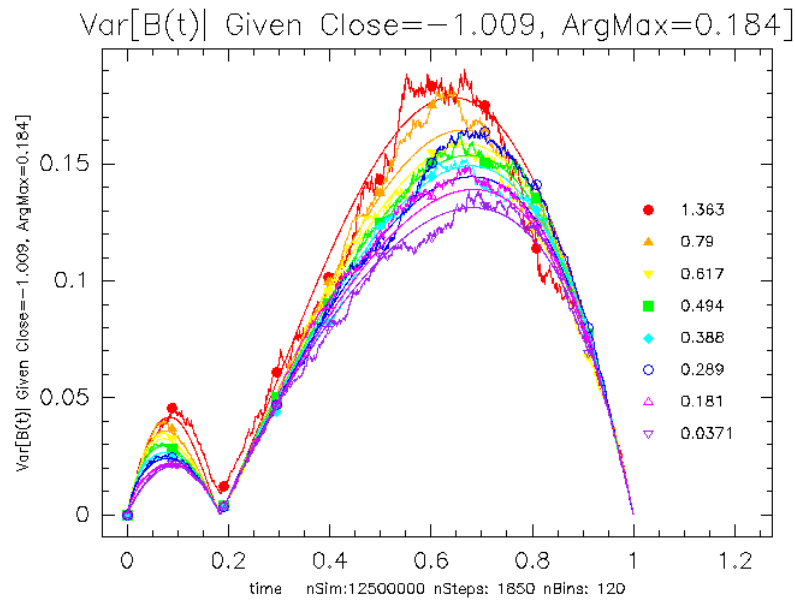


Figure 20: $\text{Var}[B(t)|\text{close}, \text{argmax}, \text{high}]$ where $\text{close} = -1.009$ and $\text{argMax} = 0.184$. Each curve is a given value of $\text{high} = \max\{B(t)\}$. The curves are bimodal with a local minimum at $t = \theta$.

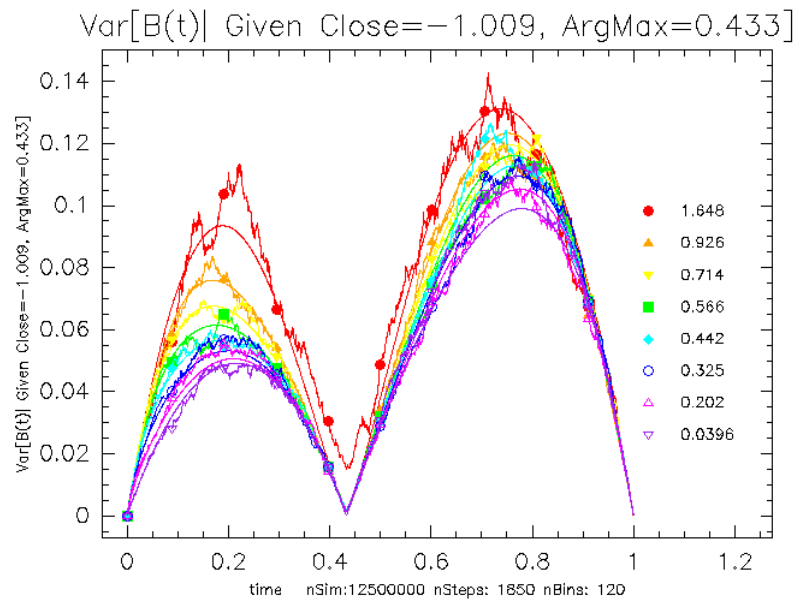


Figure 21: $\text{Var}[B(t)|\text{close}, \text{argmax}, \text{high}]$ where $\text{close} = -1.009$ and $\text{argMax} = 0.433$. The maximum of the variance is smaller when θ is larger. Since the variance is small for t near θ , the variance cannot grow as large when θ splits time into two roughly equal time intervals.

Brownian Motion Moments

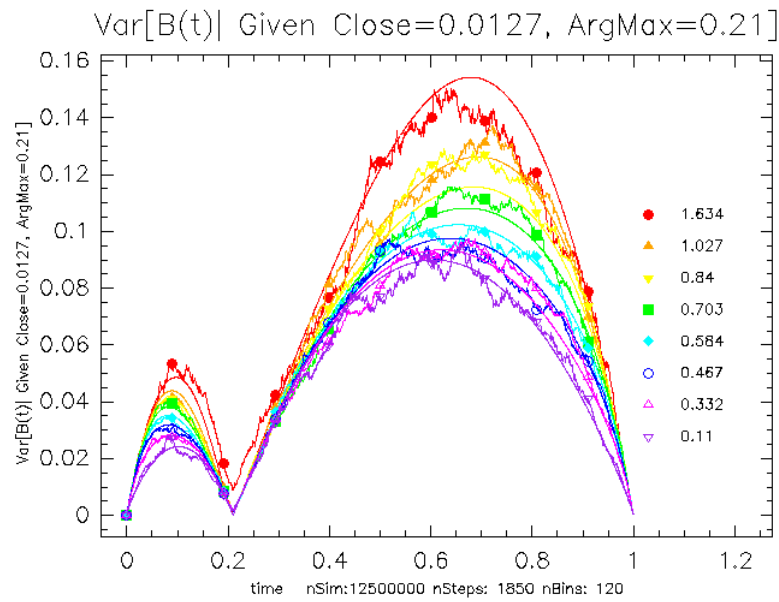


Figure 22: $Var[B(t)|close = 0.0127, \theta = 0.21, high]$ for various h values. Each curve is a given value of $high = maxB(t)$ as denoted in the legend.

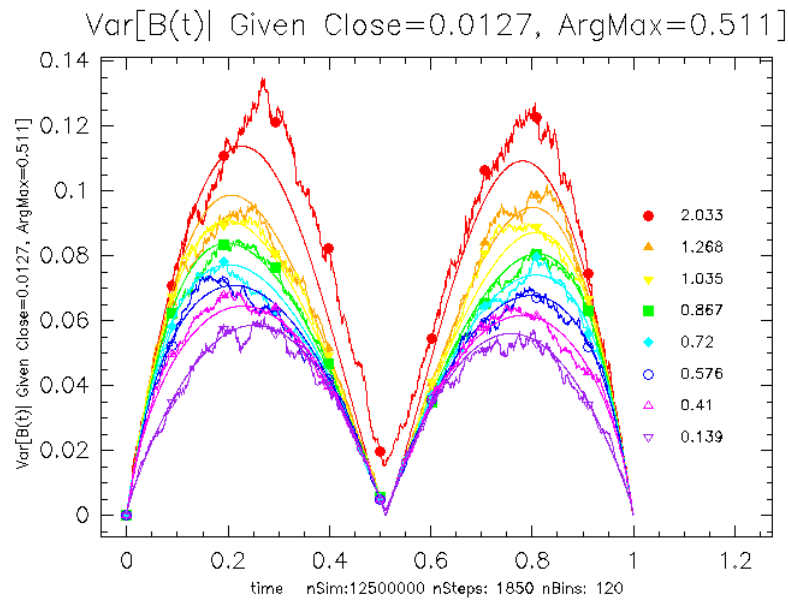


Figure 23: $Var[B(t)|close = 0.0127, \theta = 0.511, high]$. The variance is nearly symmetric in time.

13 Appendix E: Mean and Variance Given Final Value and Argmax

In the last section, we integrated over the close to calculate the moments conditional on $(high, \text{argmax})$. We now display the mean and variance of $B(t|\theta, c)$. Similar but more complicated moment calculations are possible for the case of the previous section where (θ, c) are given and one integrates over h . The figures in this section are from our simulation without the corresponding analytic calculation.

13.1 Time Dependence of Expectation given Close and Argmax

Figures 24, 25 and 26 display the expectation of $E[B(t|close, \text{argmax})]$. Each figure fixes a value of the close. The values of the close are roughly $\{-1, 0, +1\}$. The simulations use 12.5 million realizations with 1850 time steps. For each realization, we shift all of the sample paths to have the same close. For each close, the 12.5M realizations are binned into the 120 bins.

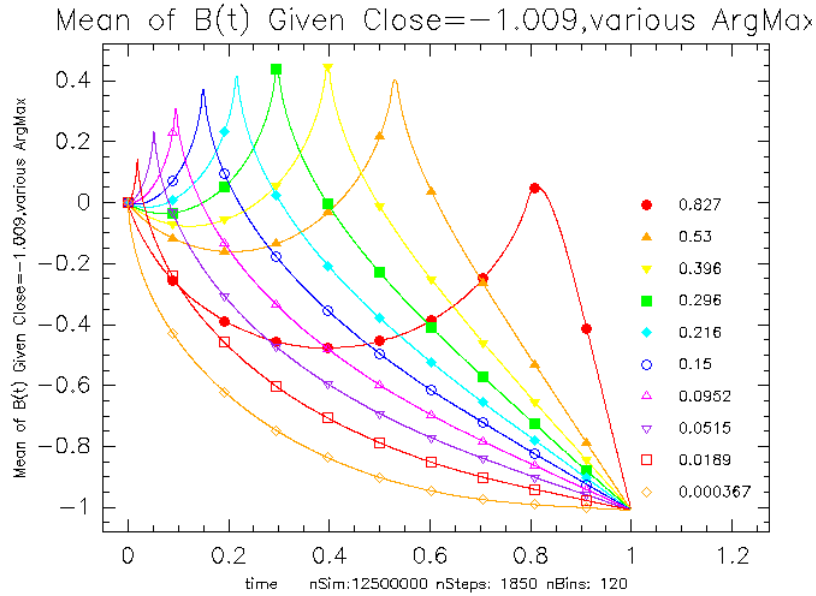


Figure 24: $E[B(t|close, \text{argmax})]$ where $close = -1.009$. Each curve is a given value of $\theta = \text{argmax}\{B\}$. Since the close is roughly at $-\sigma$, the argmax is preferentially located near zero. The expectation is peaked at $t = \theta$. The values of θ are given on the legend.

Figure 26 and Figure 24 have reflection symmetry: $E[B(t|c, \theta)] = E[B(1-t|c, 1-\theta)] - c$. This is a consequence of the reversability of Brownian motion.

13.2 Time Dependence of Variance given Close and Argmax

Figures 27, 28 and 29 display the variance of $B(t|close, \text{argmax})$. Each figure fixes a value of the close. The values of the close are roughly $\{-1, 0, +1\}$.

Figure 29 and Figure 27 have reflection symmetry: $\text{Var}[B(t|c, \theta)] = \text{Var}[B(1-t|c, 1-\theta)]$.

Brownian Motion Moments

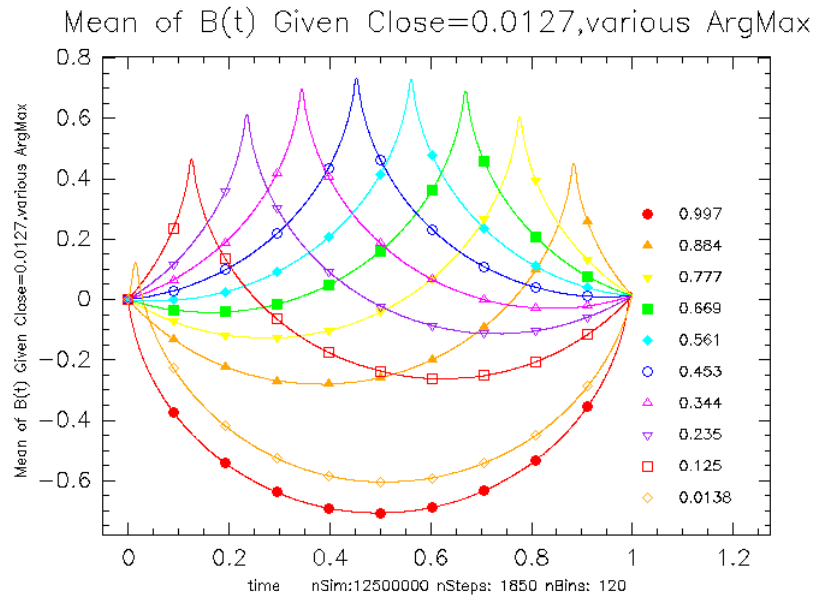


Figure 25: $E[B(t)|close, \text{argmax}]$ where $close = 0.0127$. Each curve is a given value of $\theta = \text{argmax}\{B\}$. Since the $close$ is near zero, if θ is small, the expectation after the zero-crossing resembles a semicircle.

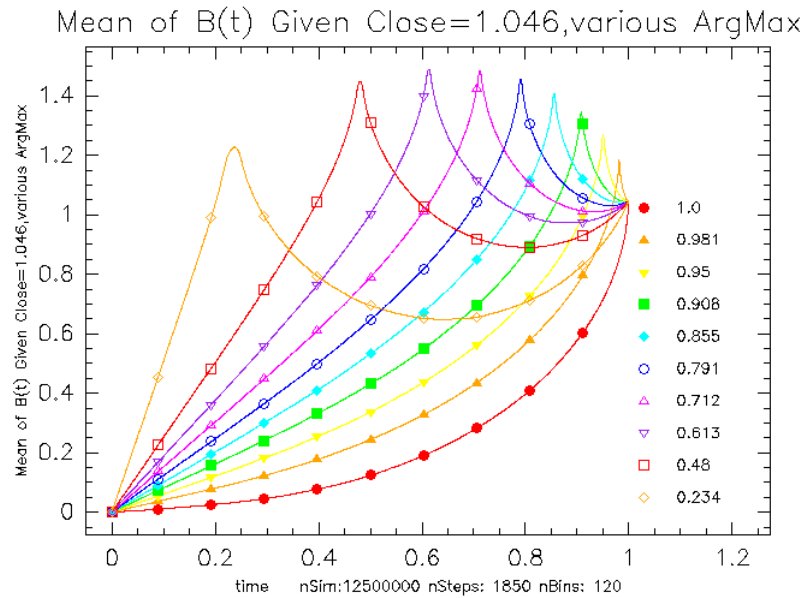


Figure 26: $E[B(t)|close = 1.046, \text{argmax}]$. Each curve is a given value of $\theta = \text{argmax}\{B\}$ as given on the legend.

Brownian Motion Moments

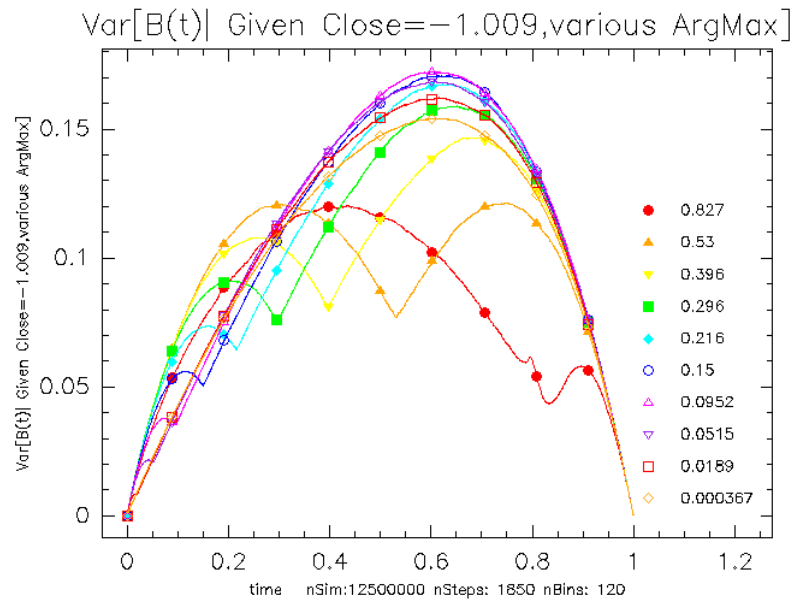


Figure 27: $Var[B(t)|close = -1.009, \text{argmax}]$ where $close = -1.009$ with the values of θ given on the legend.

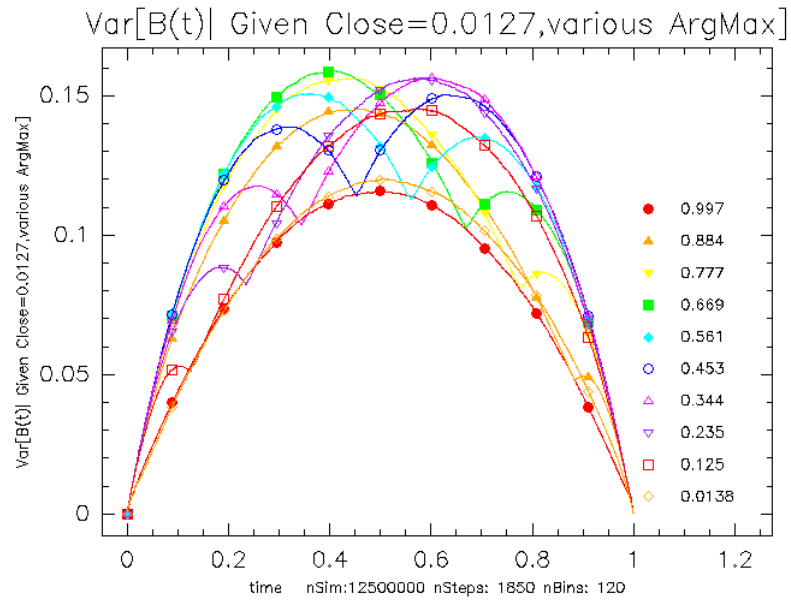


Figure 28: $Var[B(t)|close = .0127, \text{argmax}]$ where $close = 0.0127$.

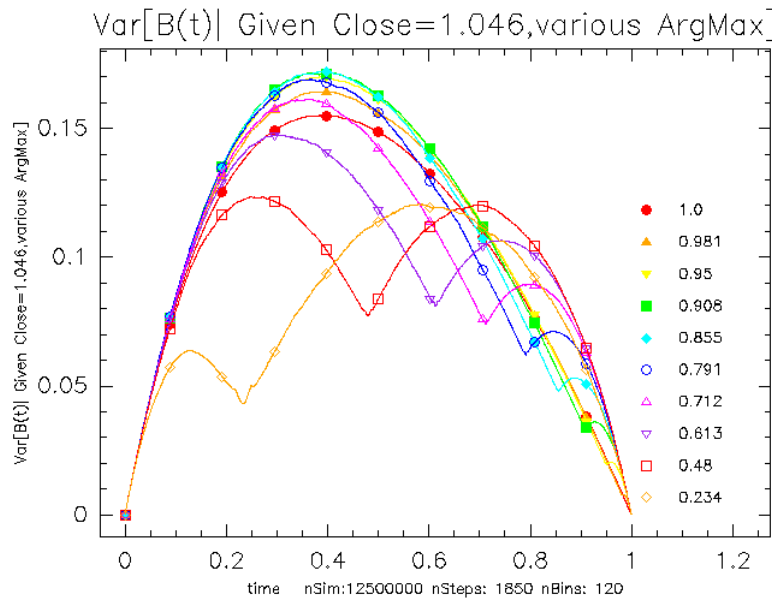


Figure 29: $Var[B(t)|close = 1.046, argmax]$ where $close = 1.046$.

References

- [1] Alabert, A. and Caballero, R.; On the minimum of a conditioned Brownian bridge. *Stochastic Models*, 2018 34, 269-291.
- [2] Belkin, B.; An invariance principle for the conditioned random walk attracted to a stable law. *Z. Wahrscheinlichkeitstheorie Gebiete*. 1972 21 45-64.
- [3] Biane, P., Le Gall, J. F. and Yor, M.; Un processus qui ressemble au pont Brownien. *Séminaire de probabilités de Strasbourg*, Springer-Verlag, Berlin Heidelberg New York, 1987.
- [4] Borodin, A.N. and Salminen, P.; *Handbook of Brownian Motion: Facts and Formulae*. Birkhäuser, Basel 2002 MR-1477407.
- [5] Choi B. and Roh J.; On the trivariate joint distribution of Brownian motion and its maximum and minimum. *Statistics and Probability Letters* 83, 1046-1053.
- [6] Denisov, I. V.; A random walk and a Wiener process near a maximum. *Theor. Prob. Appl.*, 1984, 28 821-824. *Math. Review* MR-85f:60117.
- [7] Devroye, L.; On exact simulation algorithms for some distributions related to Brownian motion and Brownian meanders. *Recent developments in Applied Probability and Statistics*, 2010 pp. 1-35, Physica-Verlag HD.
- [8] Durrett, R. T., Iglehart, D. L. and Miller, D. R.; Weak convergence to Brownian meander and Brownian excursion, *Ann. Probability*, 1977 5 no. 1, 117-129. MR-55:9300.
- [9] Durrett, R. T. and Iglehart, D. L.; Functionals of Brownian Meander and Brownian Excursion. *The Annals of Probability*, Probability, 1977 5, No. 1, 130-135.
- [10] Imhof, J. P.; Density factorizations for Brownian motion, meander and the three-dimensional Bessel process, and applications. *J. Appl. Probab.*, 1984, 21 500-510. *Math. Review* MR-85j:60152.
- [11] Imhof, J. P.; On Brownian bridge and excursion. *Studia Sci. Math. Hungar.*, 1985 20 1-10. *Math. Review* MR-88h:60159.
- [12] Itô, K. and McKean, H.; *Diffusion Processes and their Sample Paths*. Springer-Verlag, New York. 1965.
- [13] Karatzas, I. and Shreve, S. E.; *Brownian Motion and Stochastic Calculus*. Second Edition, Springer, New York, 1998, 'MR1121940.
- [14] Lévy, P.; *Processus Stochastiques et Mouvement Brownien*. Gauthier-Villars, Paris, 1948 MR-0190953.

- [15] McLeish D. L.; Highs and lows: Some properties of the extremes of a diffusion and applications in finance. *Canadian Journal of Statistics*, 2002 *30*, 243-267.
- [16] Pitman J. and Yor M.; Decomposition at the maximum for excursions and bridges of one-dimensional diffusions. In N. Ikeda, S. Watanabe, M. Fukushima, and H. Kunita, editors, *Ito's Stochastic Calculus and Probability Theory*, pages 293-310. Springer. *Lecture Notes in Math.* 851. 1996 MR-98f:60153.
- [17] Riedel, K. S.; The Value of the High, Low and Close in the Estimation of Brownian Motion. *Statistical Inference for Stochastic Processes* 2020. Also <https://arxiv.org/abs/1911.05280>
- [18] Riedel, K. S.; Mean and variance of Brownian motion with given final value, maximum and argmax: Extended version. <https://arxiv.org/pdf/1911.05272.pdf> 2020.
- [19] Shepp, L. A.; The joint density of the maximum and its location for a Wiener process with drift. *Journal of Applied Probability*, 1979 *16*, 423-427
- [20] Williams, D.; Decomposing the Brownian path. *Bull. Amer. Math. Soc.*, 1970 *76*:871-873. *Math. Review* MR-41.
- [21] Williams, D.; Path decomposition and continuity of local time for one dimensional diffusions I. *Proc. London Math. Soc.* 1974 *28*:738-768. *Math. Review* MR-50.
- [22] Yor M.; Some Remarks about the joint law of Brownian motion and its supremum. *Seminar de Probabilitèes, Strasbourg*, 1997 *31* 306-314.

Acknowledgments. The author thanks his referees for their helpful remarks.